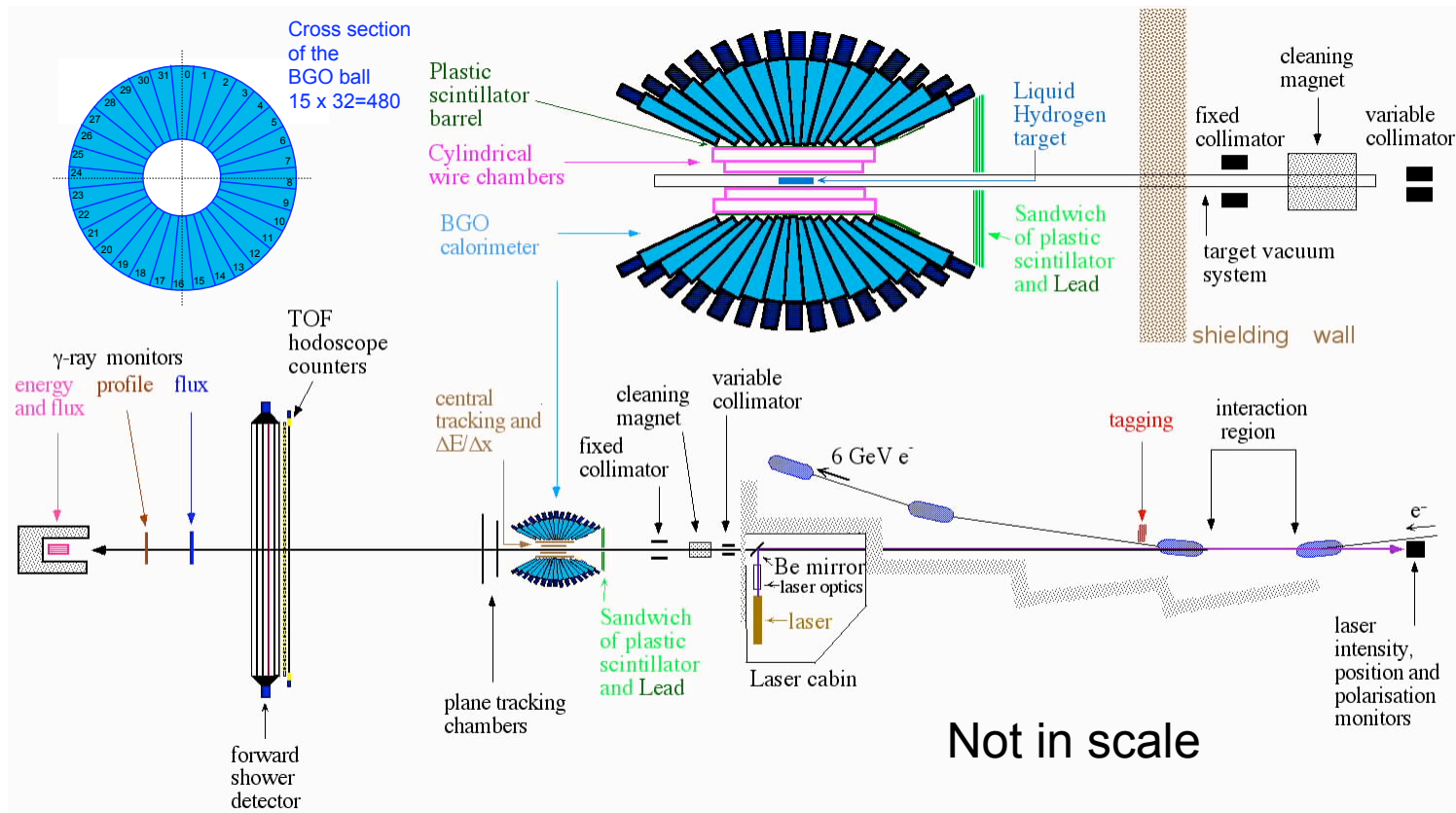


# The Graal experiment at the ESRF

Carlo Schaerf  
for the  
Graal Collaboration

University of Rome “Tor Vergata”  
and  
INFN - Sezione di Roma Tor Vergata

# The Graal Apparatus



# The Graal Detector

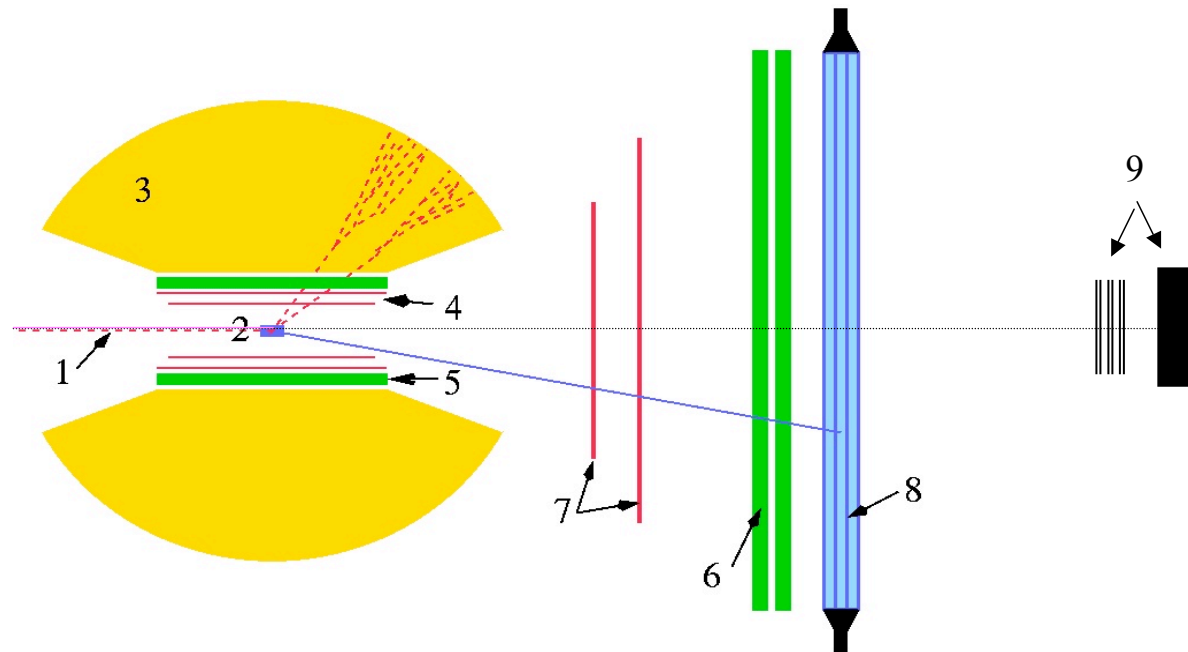
➤ Liquid Target :  
2 H<sup>2</sup> or D<sup>2</sup>

➤ Central angles :  
 $25^\circ < \theta < 155^\circ$

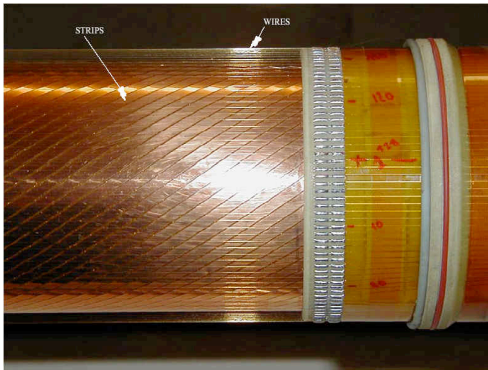
➤ Forward angles :  
 $\theta < 25^\circ$

- 6 BGO calorimeter
- 7 2 cylindrical MWPC
- 8 barrel of plastic scintillators

- 6 double wall of scintillators
- 7 planar MWPC
- 8 shower wall
- 9 monitor detectors



## Central Angles ( $25^\circ < \theta < 155^\circ$ ): MWPC, BARREL



- **2 cylindrical MWPC**

tracking of the charged particles

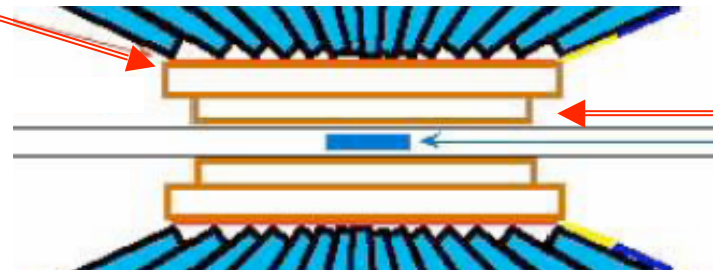
Angular resolution  $\Delta\theta = 2^\circ$   
 $\Delta\phi = 1.4^\circ$

Around the MWPC:

- **barrel of 32 plastic scintillators (NE102A)**



charged/neutral particles  
discrimination  
(veto for neutral particle)  
charged particles identification  
by means of  $dE/dx$  vs.  $E$   
( $E$  is measured in the BGO)



## Forward Angles ( $\theta < 25^\circ$ ): MWPC, Hodoscope

- 2 sets of planar MWPC (xy, uv)

tracking of the charged particles

Angular resolution

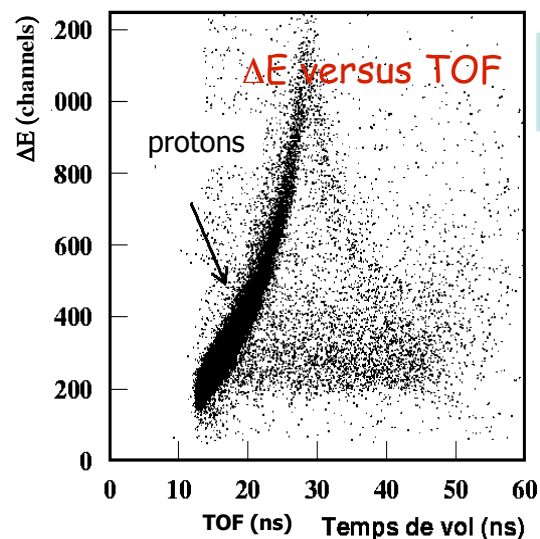
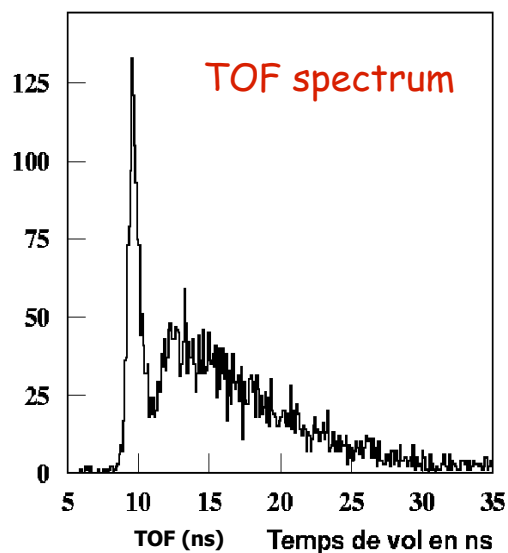
$$\Delta\theta = 2^\circ$$

$$\Delta\phi = 1.4^\circ$$

- Double Forward Scintillator Wall (hodoscope)

26 x 26 bars NE110A  
300 x 11,5 x 3 mm

- Charged particle identification (pions, proton) by means  $\Delta E$  vs. TOF
- TOF measurement for energy determination of charged particles



Angular resolution

$$\Delta\theta \cong \Delta\varphi \cong 3^\circ$$

## Forward Angles ( $\theta < 25^\circ$ ): Russian Wall

- **Forward Shower Wall**

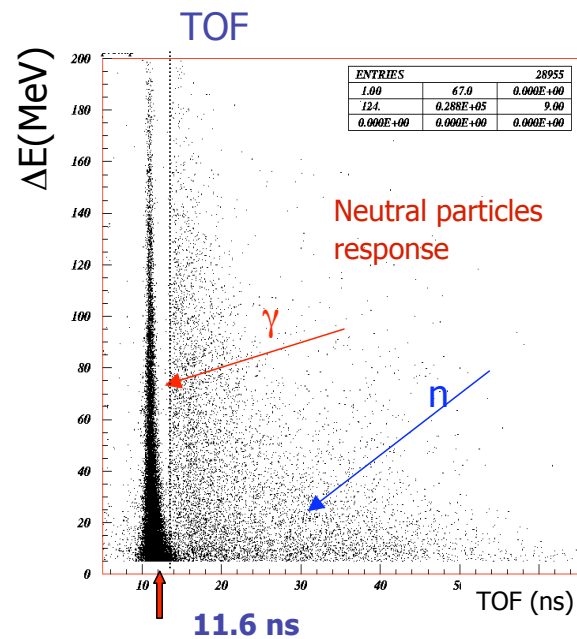
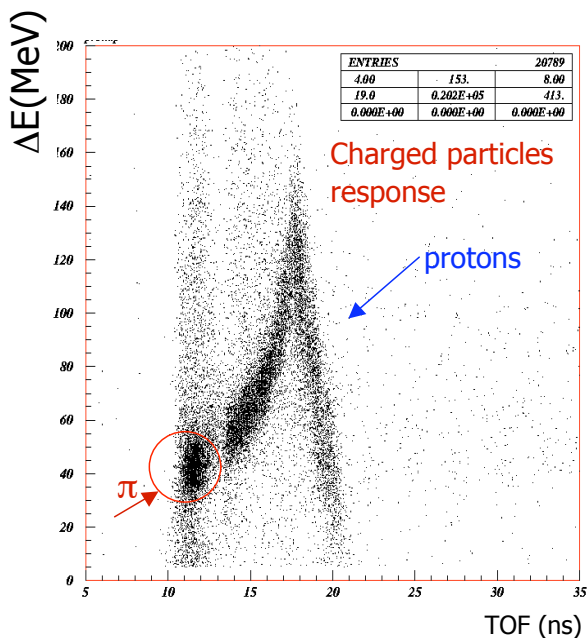
TOF measurements provide:

- ✓ Energy information for protons and neutrons
- ✓ photon/neutron discrimination
- ✓ pion/proton discrimination
- ✓ charged/neutral particle discrimination in coincidence with the hodoscope

16 *sandwich* modules :

- 4 layers of scintillators 10 cm thick
- 3 layers of lead converters 3 mm thick
- frontal iron plate 5 mm thick

photon efficiency 92-95%  
neutron efficiency 22%



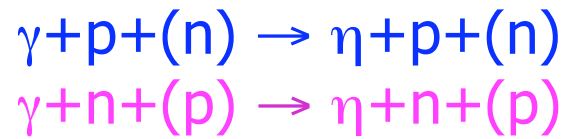
Sep-16-09

Carlo Schaerf - Moscow - EMIN 090917

6

## A brief report

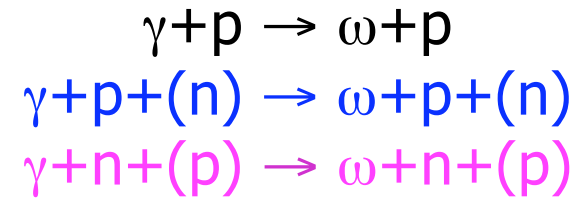
$\eta$  photo-production in  $D_2$   
on quasi free proton  
on quasi free neutron



total photo-production  
cross sections

INR

$\omega$  photo-production in  $H_2$  and  $D_2$   
on free proton in  $H_2$   
on quasi free proton in  $D_2$   
on quasi free neutron in  $D_2$



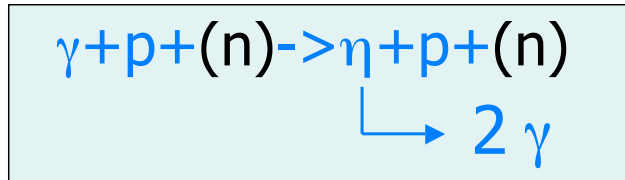
$\pi^- p$  photo-production in  $D_2$



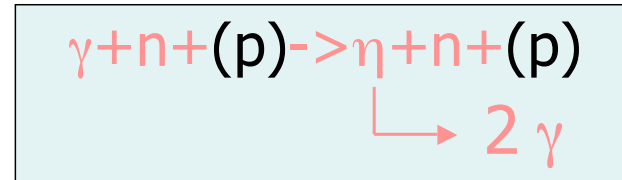
## Events Selection for $\eta$ Photoproduction on Quasi-Free Nucleons from Deuteron

$\eta$  photo-production on quasi free proton

$\eta$  photo-production on quasi free neutron



**Neutron is a spectator**



**Proton is a spectator**

**2  $\gamma$  in the BGO  
+  
participant nucleon in the central or forward  
direction**

**NO other particle  
(the spectator particle is not detected)**



# Bi-Dimensional Cuts

**Over-determined Information provided by apparatus**

Particles energy and angles can be Measured or calculated by the Variables of the other particles from two-body kinematics

$$\left. \begin{matrix} E_{\bar{\gamma}} \\ E_{\eta}^{meas} & \theta_{\eta}^{meas} & \varphi_{\eta}^{meas} \\ & \theta_N^{meas} & \varphi_N^{meas} \end{matrix} \right\} \rightarrow \begin{matrix} \theta_N^{calc} \\ E_{\eta}^{calc} \\ M_{\eta}^{miss} \end{matrix}$$

Bi-dimensional distributions

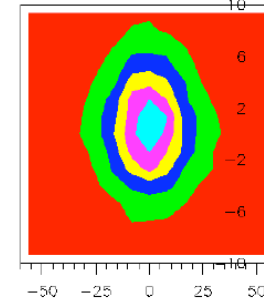
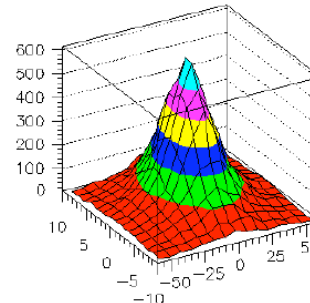
Each Distribution fitted by Bi-dimensional Gaussian

extraction of mean and  $\sigma_i$  values

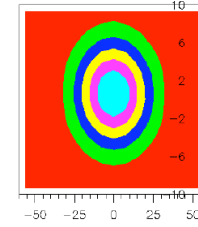
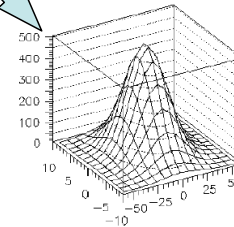
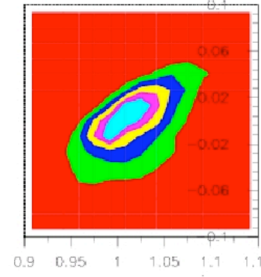
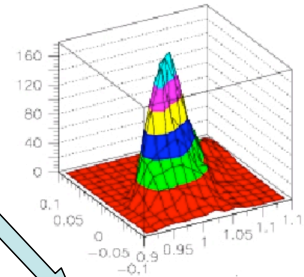
$$\frac{(x - \mu_1)^2}{\sigma_1^2} + \frac{(x - \mu_2)^2}{\sigma_2^2} - \frac{2C(x - \mu_1)(x - \mu_2)}{\sigma_1\sigma_2} < \sigma^2 \quad [\sigma = 1 - 3]$$

Selection cuts:

$$(\theta_N^{meas} - \theta_N^{calc}) \text{ vs } (\varphi_N^{meas} - \varphi_{\eta}^{meas} - 180^\circ)$$



$$(E_{\eta}^{calc} / E_{\eta}^{meas}) \text{ vs } (M_{\eta}^{miss} - M_N)$$



# Events Selection – Quasi Two-Body Kinematics

Quasi-free process  
and low Fermi momentum



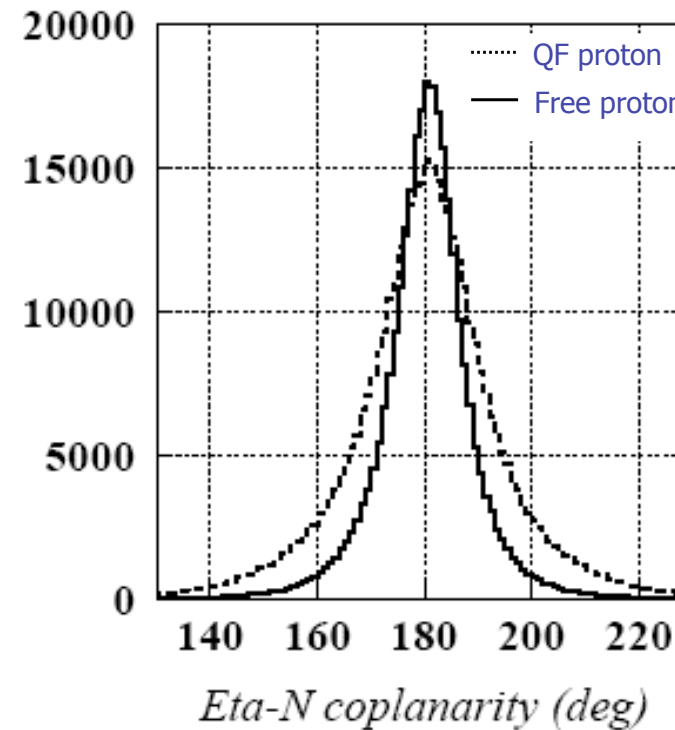
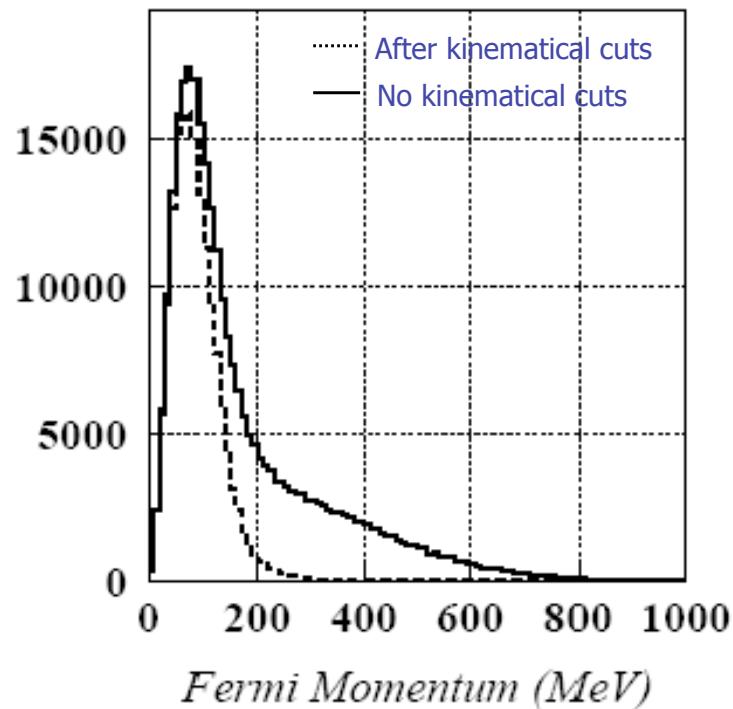
## Kinematical Analysis:

- Two-body nature of each reaction step:

## Fermi momentum Contribution



## Smearing of distributions



# $\eta$ Invariant Mass and Estimated Background After Cuts

a) Central proton

2.4 %

b) Central neutron

3.9 %

c) Forward proton

0.9 %

d) Forward neutron

1.4 %

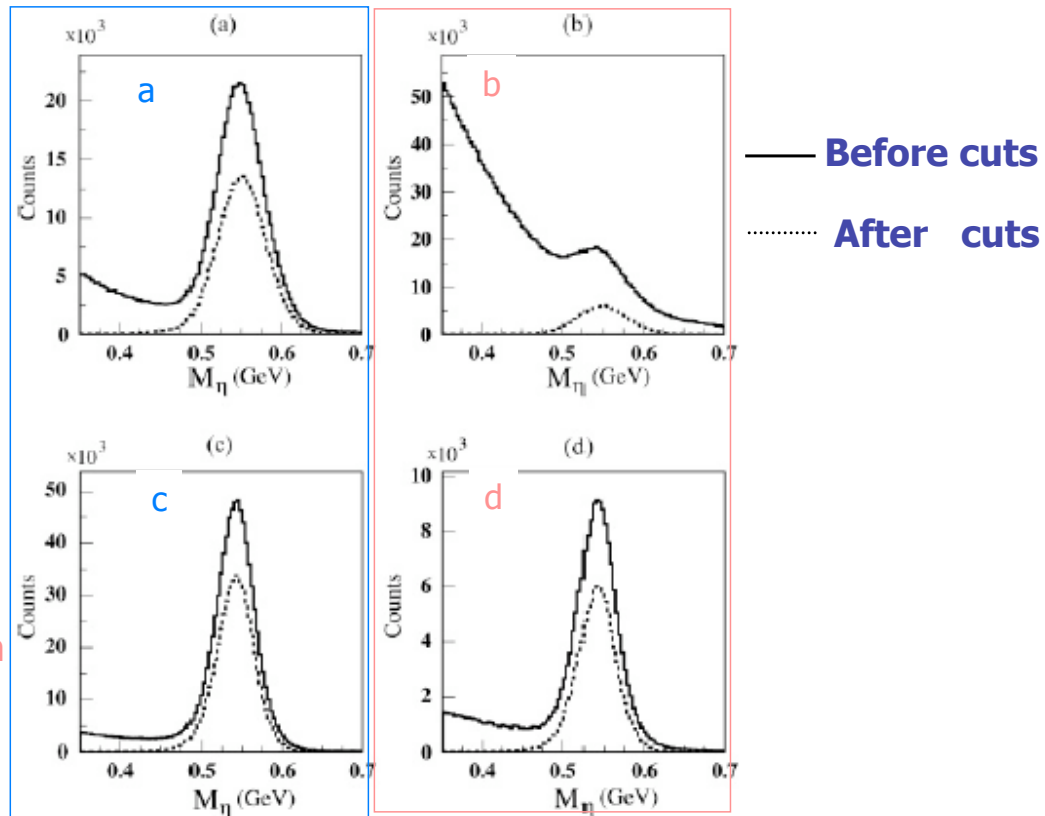
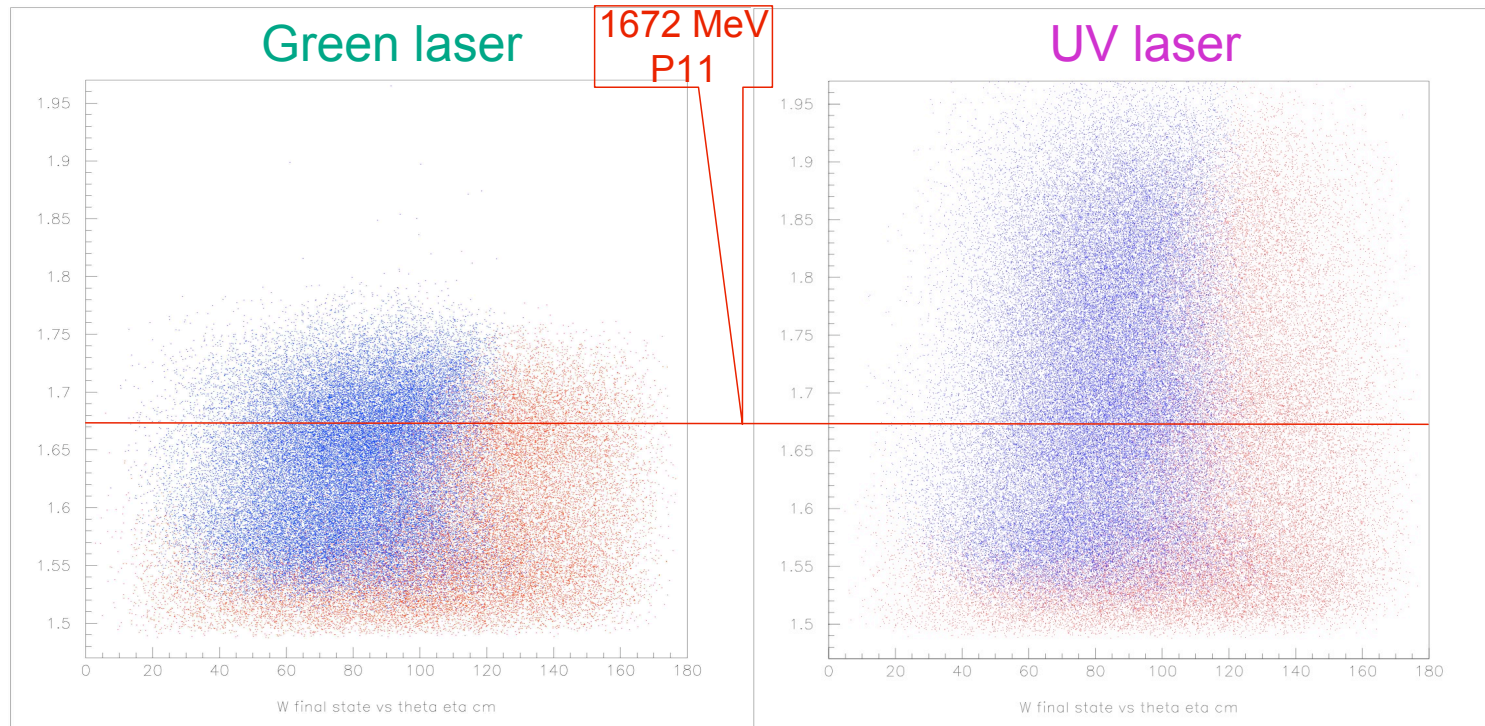


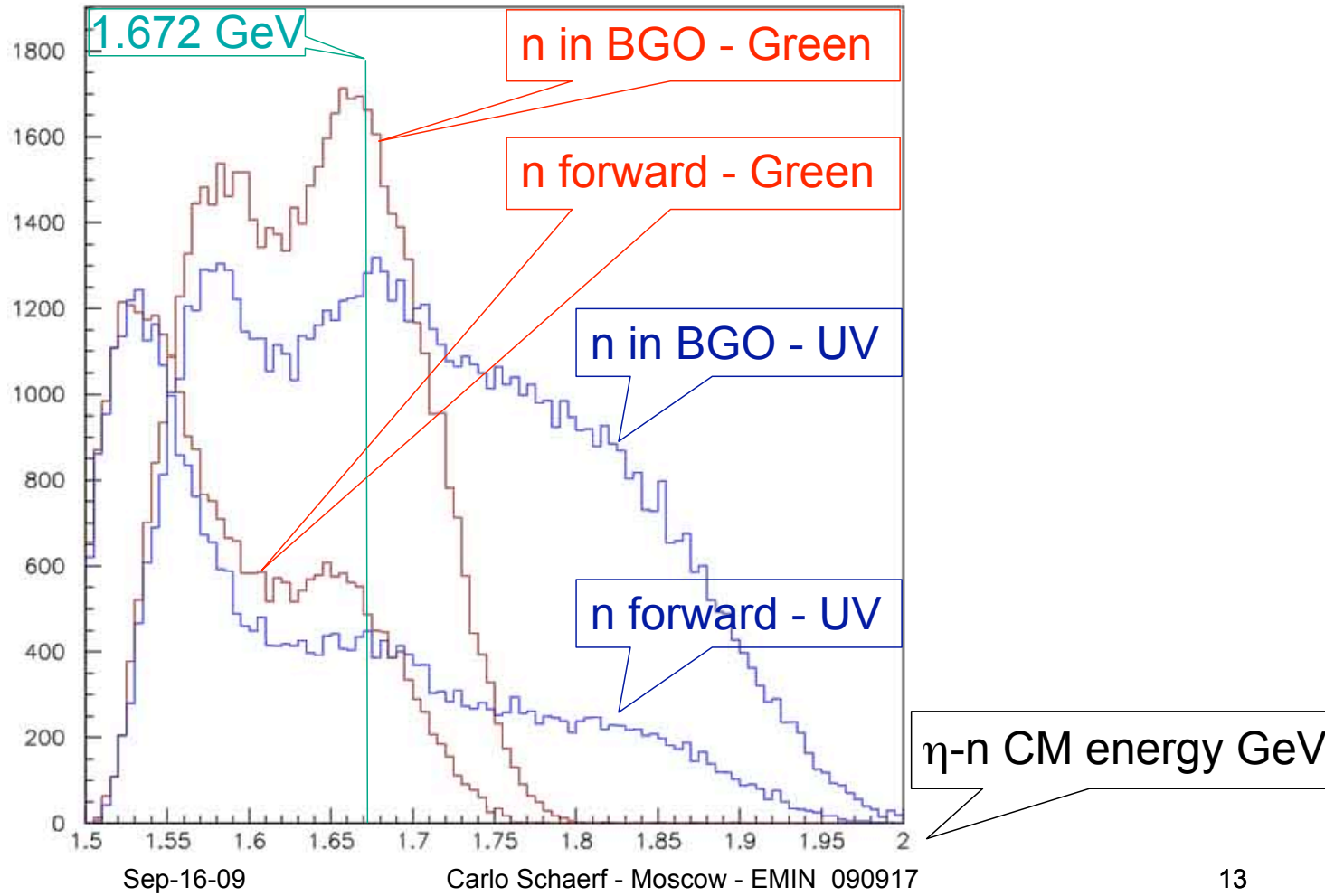
FIG. 4. The  $\eta$  invariant mass without cuts (solid line) and with the kinematical cuts (dotted line) for (a) a proton and (b) a neutron in the central region and for (c) a proton and (d) a neutron in the forward direction.

$w(\text{fin})$  vs  $\theta_{\eta}^{\text{cm}}$

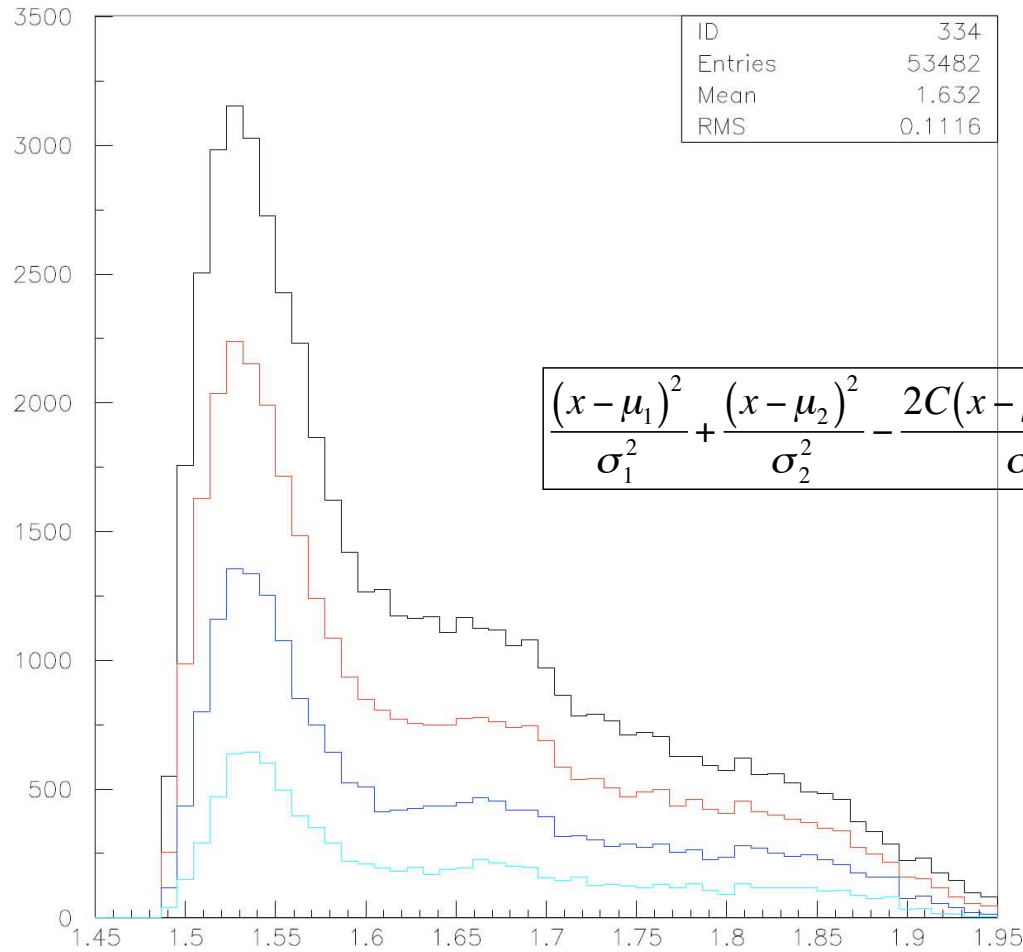


red neutron forward  
blue neutron in BGO

# GREEN vs UV & Forward vs BGO



# Yield vs sigma: Forward n



Bidimensional cuts

$\sigma = 3$      $\sigma^2 = 9$

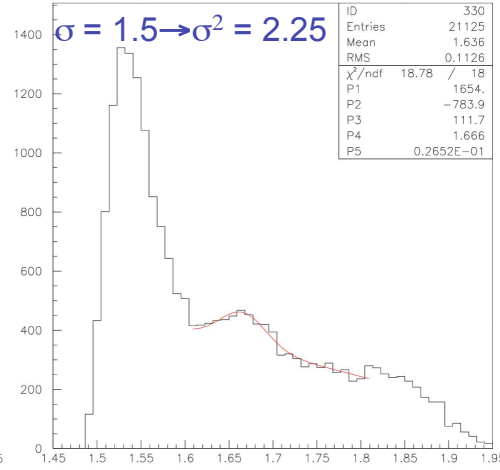
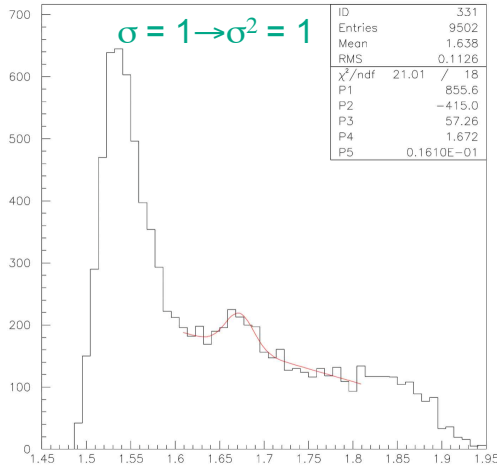
$\sigma = 2$      $\sigma^2 = 4$

$\sigma = 1.5$      $\sigma^2 = 2.25$

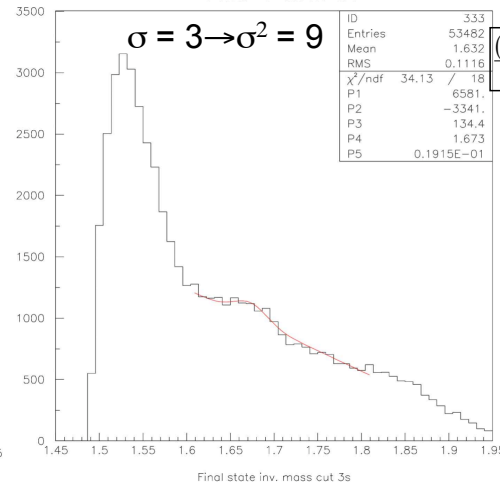
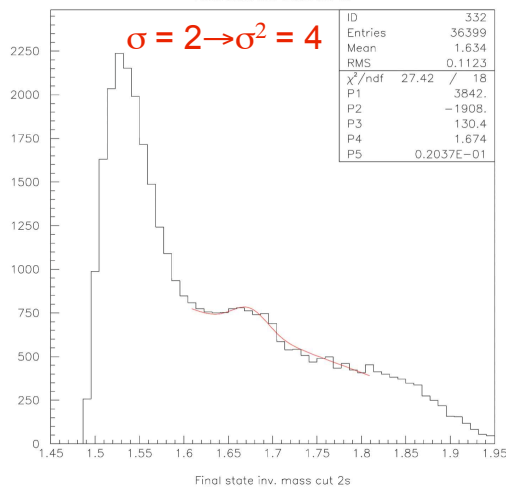
$\sigma = 1$      $\sigma^2 = 1$

$$\frac{(x - \mu_1)^2}{\sigma_1^2} + \frac{(x - \mu_2)^2}{\sigma_2^2} - \frac{2C(x - \mu_1)(x - \mu_2)}{\sigma_1\sigma_2} < \sigma^2 \quad [\sigma = 1 - 3]$$

# Resonance Width as a Function of Sigma: Forward n UV

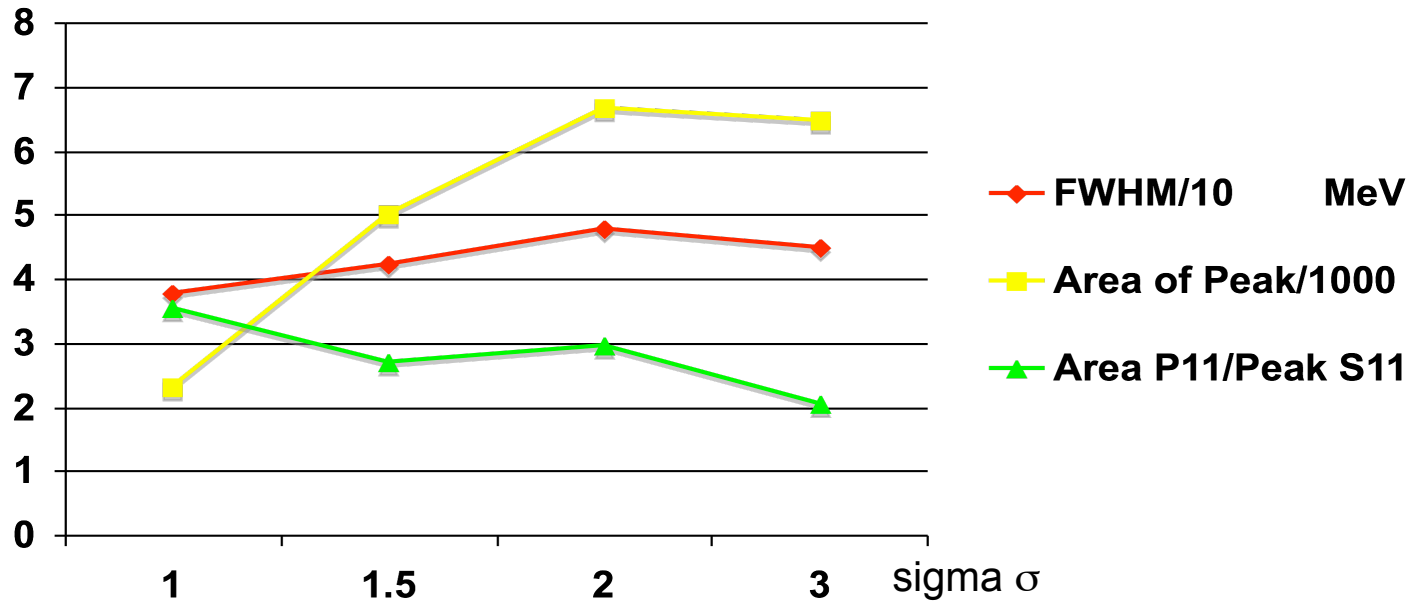


Linear fit + Gaussian:  
 P3 = gaussian height  
 P4 = gaussian center  
 P5 = gaussian width (rms)  
 Resonance position:  
 $W=P4$   
 Resonance width (FWHM):  
 $D = 2,34 \cdot P5$   
 Resonance Strenght:  
 $A=P3 \cdot P5$



$$\frac{(x-\mu_1)^2}{\sigma_1^2} + \frac{(x-\mu_2)^2}{\sigma_2^2} - \frac{2C(x-\mu_1)(x-\mu_2)}{\sigma_1\sigma_2} < \sigma^2 \quad [\sigma = 1-3]$$

## Resonance Width as a Function of Sigma: Forward n UV

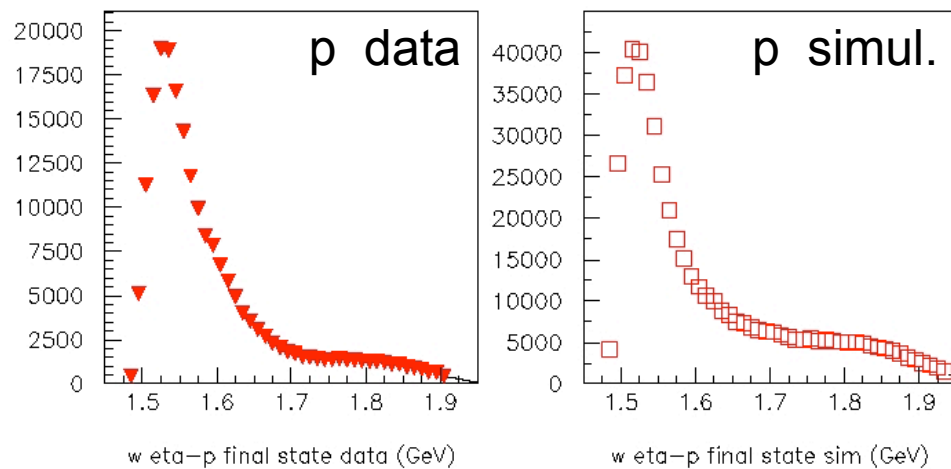
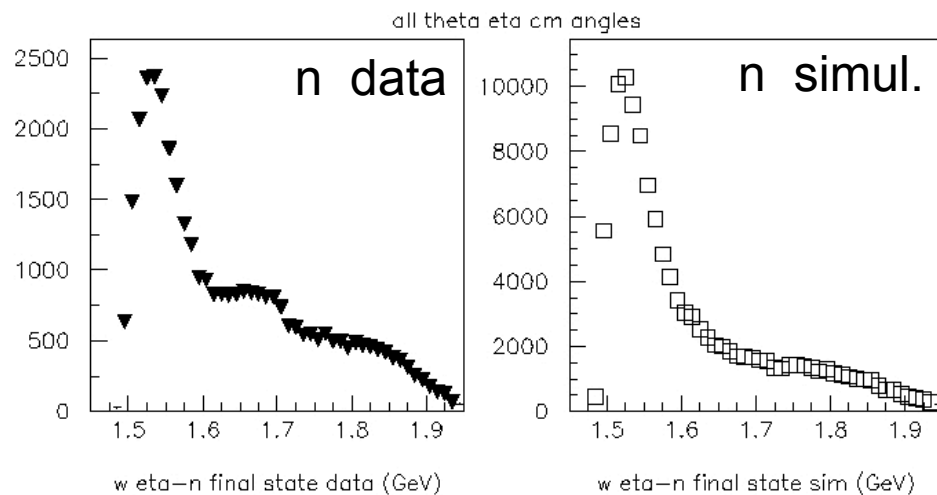


$\sigma$ sigma	$\sigma^2$	P3 Gaussian Height Counts	P4 Gaussian Center W GeV	P5 Gaussian Width (rms) MeV	$\Gamma \approx \text{FWHM}$ $2.36 * 0.1 * P5$ MeV/10	Area of peak = $(2\pi)^{1/2} * P5 * P3$ Counts*MeV	S11 Peak Counts	Area of P11 /Peak of S11 MeV	Area of Peak/1000 Counts*MeV
1,00	1,00	57,26	1,672	16,10	3,77	2310,80	650,00	3,56	2,31
1,50	2,25	110,30	1,670	18,10	4,24	5004,25	1850,00	2,71	5,00
2,00	4,00	130,40	1,674	20,40	4,77	6667,96	2250,00	2,96	6,67
3,00	9,00	134,40	1,673	19,20	4,49	6468,23	3170,00	2,04	6,47

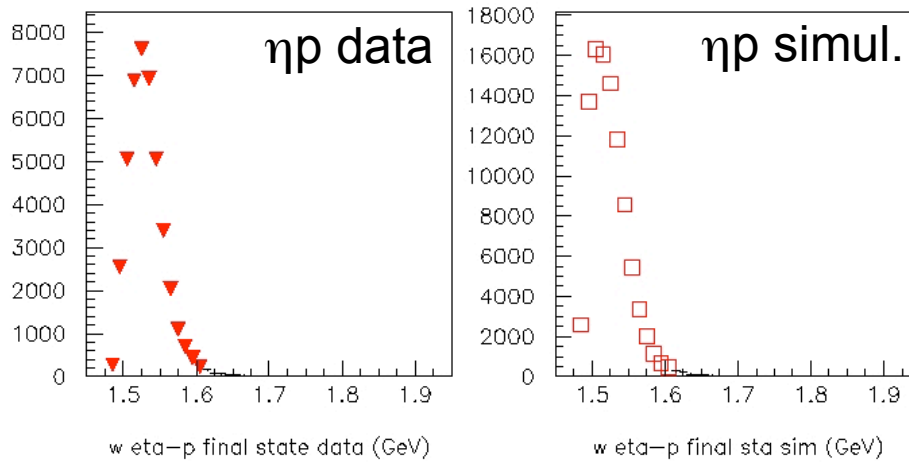
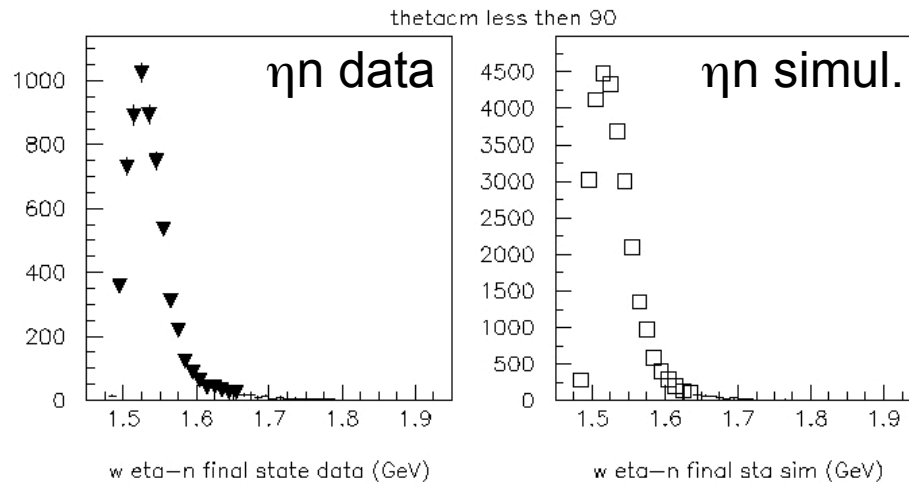
$$W = 1672 \text{ MeV} \Rightarrow k = 1018 \text{ MeV}$$



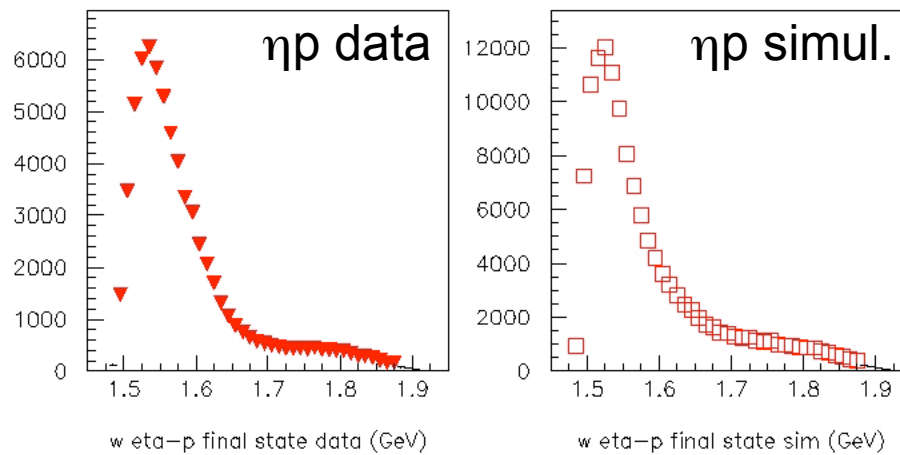
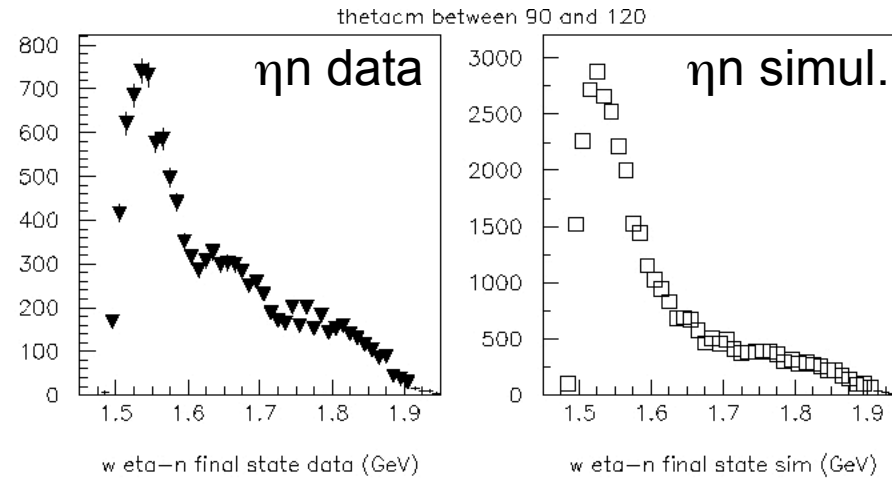
# $\eta$ -n Yield for all angles – Forward neutron – $\theta_{n\text{Lab}} < 25^\circ$



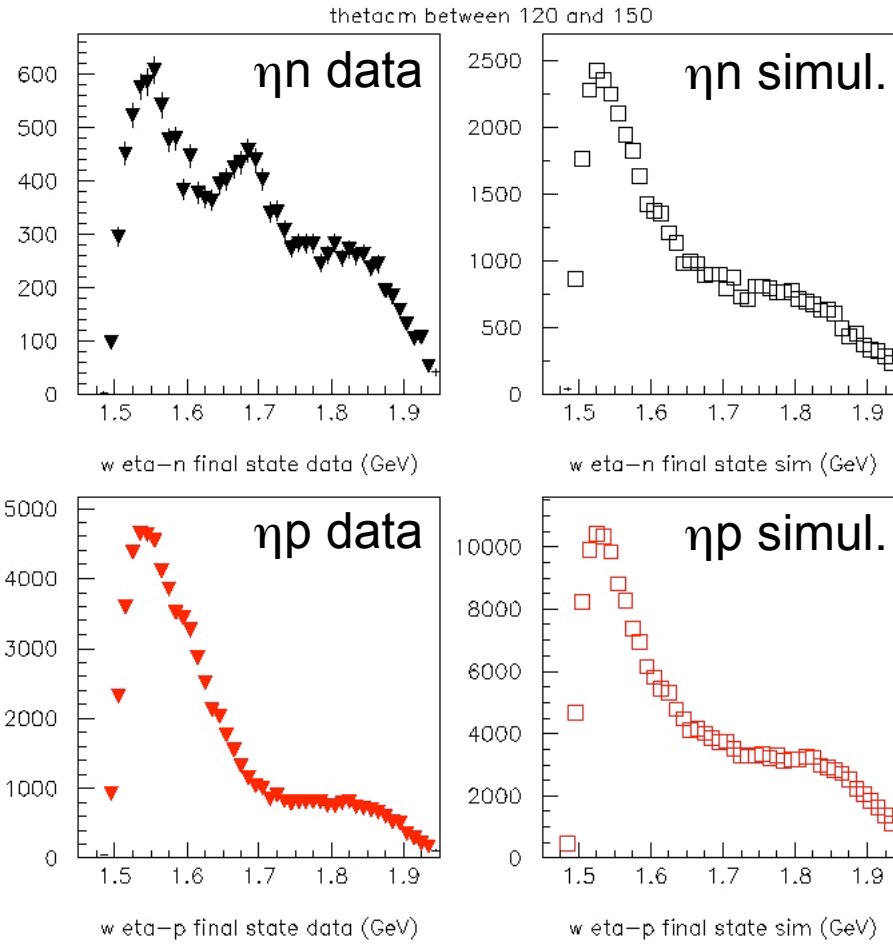
# $\eta$ -n Yield for $\theta_\eta < 90^\circ$



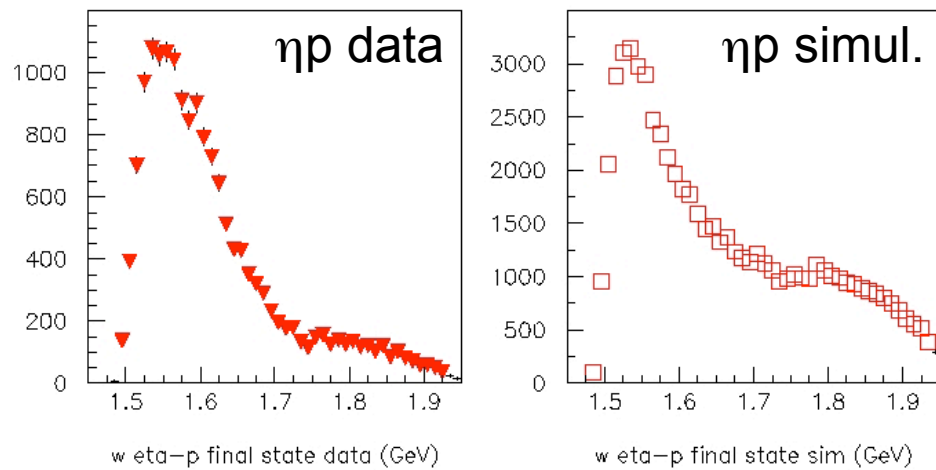
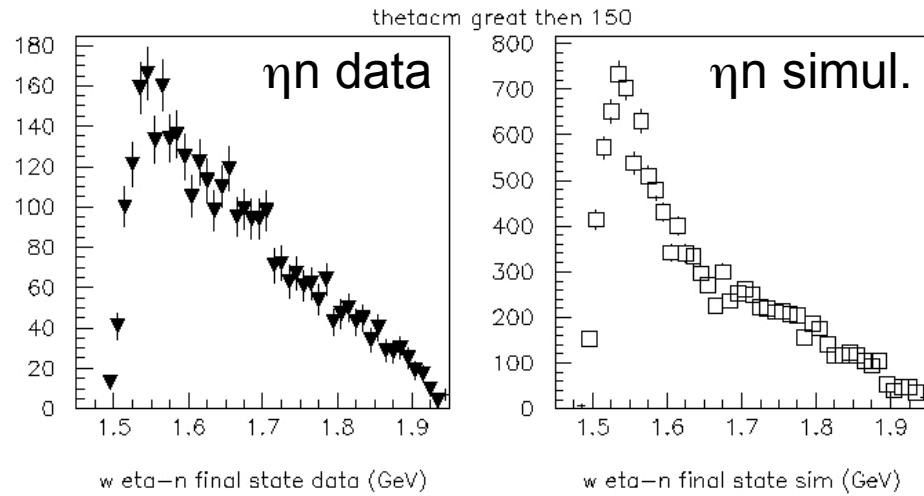
# $\eta$ -n Yield for $\theta_\eta = 90^\circ - 120^\circ$



# $\eta$ -n Yield for $\theta_\eta = 120^\circ - 150^\circ$



# $\eta$ -n Yield for $\theta_\eta > 150^\circ$



# THE BEAM ASYMMETRY

Selected events grouped in  
Fixed  $E_\gamma$ ,  $\theta_\eta^{cm}$ ,  $\phi_\eta^{cm}$  bins

**11  $E_\gamma$  bins**  
**16  $\phi_\eta^{cm}$  bins**  
**8  $\theta_\eta^{cm}$  bins**

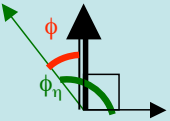
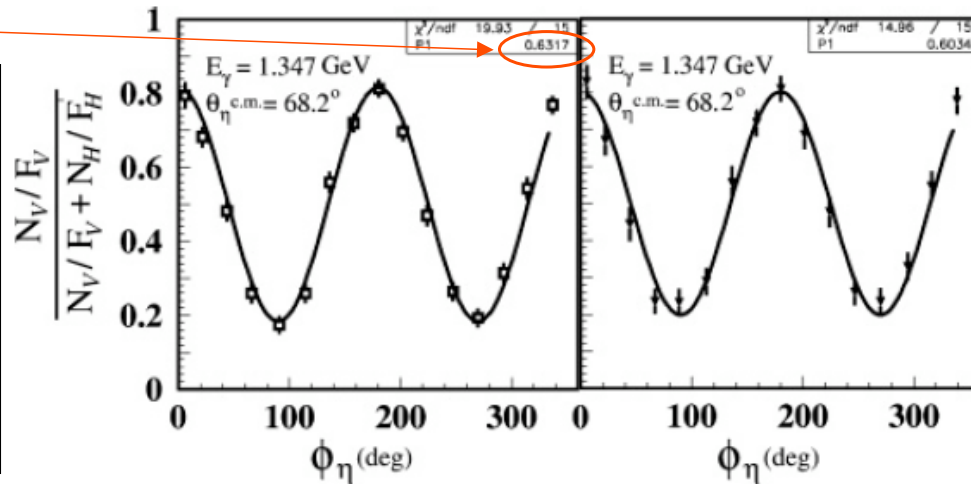
$P\Sigma$   
free parameter in the fit

For each  $(E_\gamma, \theta_\eta^{cm}) \Rightarrow$  Fit of azimuthal  
behavior of the ratio:

$$\frac{N_V / K_V}{N_V / K_V + N_H / K_H} = \frac{1}{2} \left[ 1 + P \Sigma \cos(2\phi_\eta) \right]$$

$N_{V,H}$  = Number of selected events with vertical/horizontal beam polarization  
 $K_{V,H}$  = Flux corresponding to vertical/horizontal beam polarization  
 $P$  = Polarization degree of the beam at the bin mean energy  
 $\Sigma$  = Beam asymmetry to be determined for every  $(E_\gamma, \theta_\eta^{cm})$

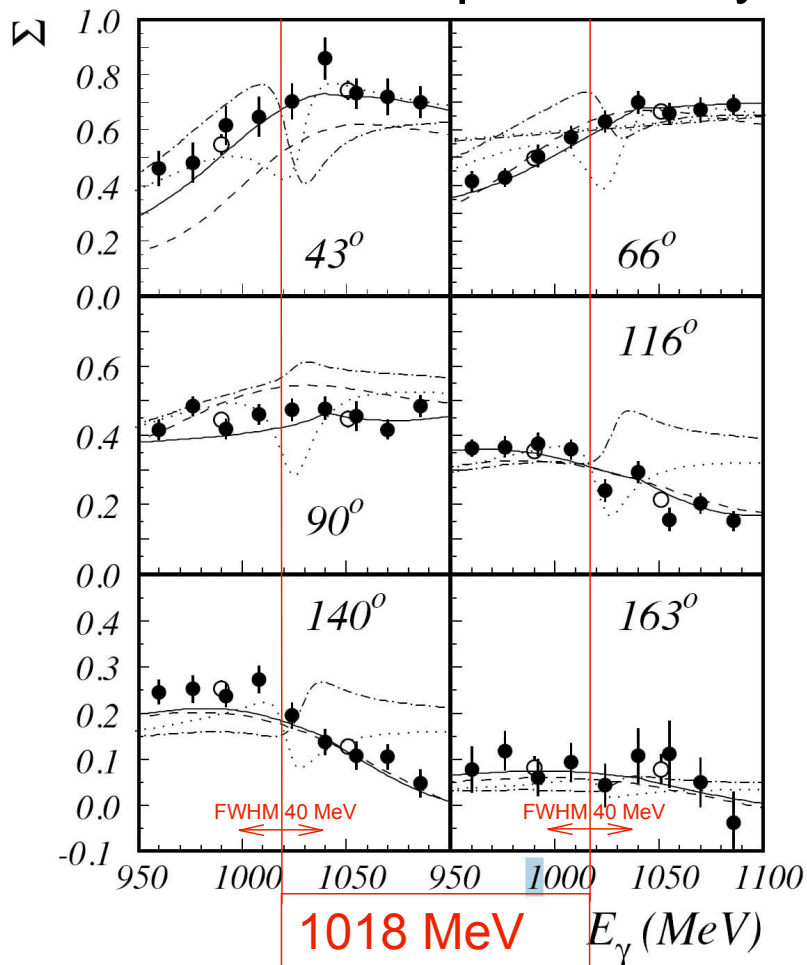
**NB:**  
The + sign in front of  $P\Sigma\cos(2\phi_\eta)$  term in the distribution is due to the coordinate system choice.  
If  $\phi$  is the angle between the reaction plan and the polarization direction of the photon and  $\phi_\eta$  is the azimuthal angle of outgoing meson, we have:

**QF-PROTON DATA**

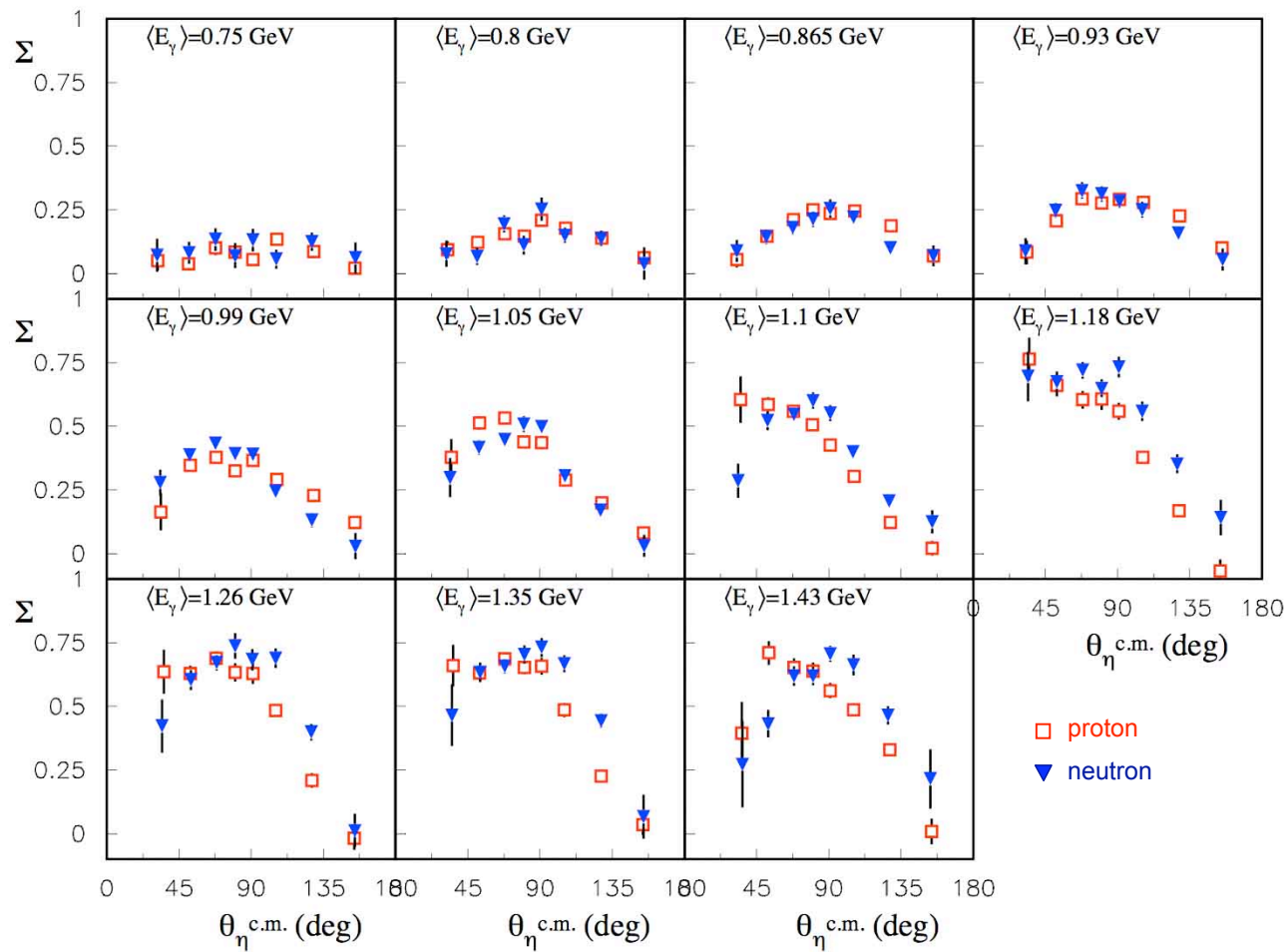
**QF-NEUTRON DATA**

## $\eta$ Asimmetry $\Sigma$ free p



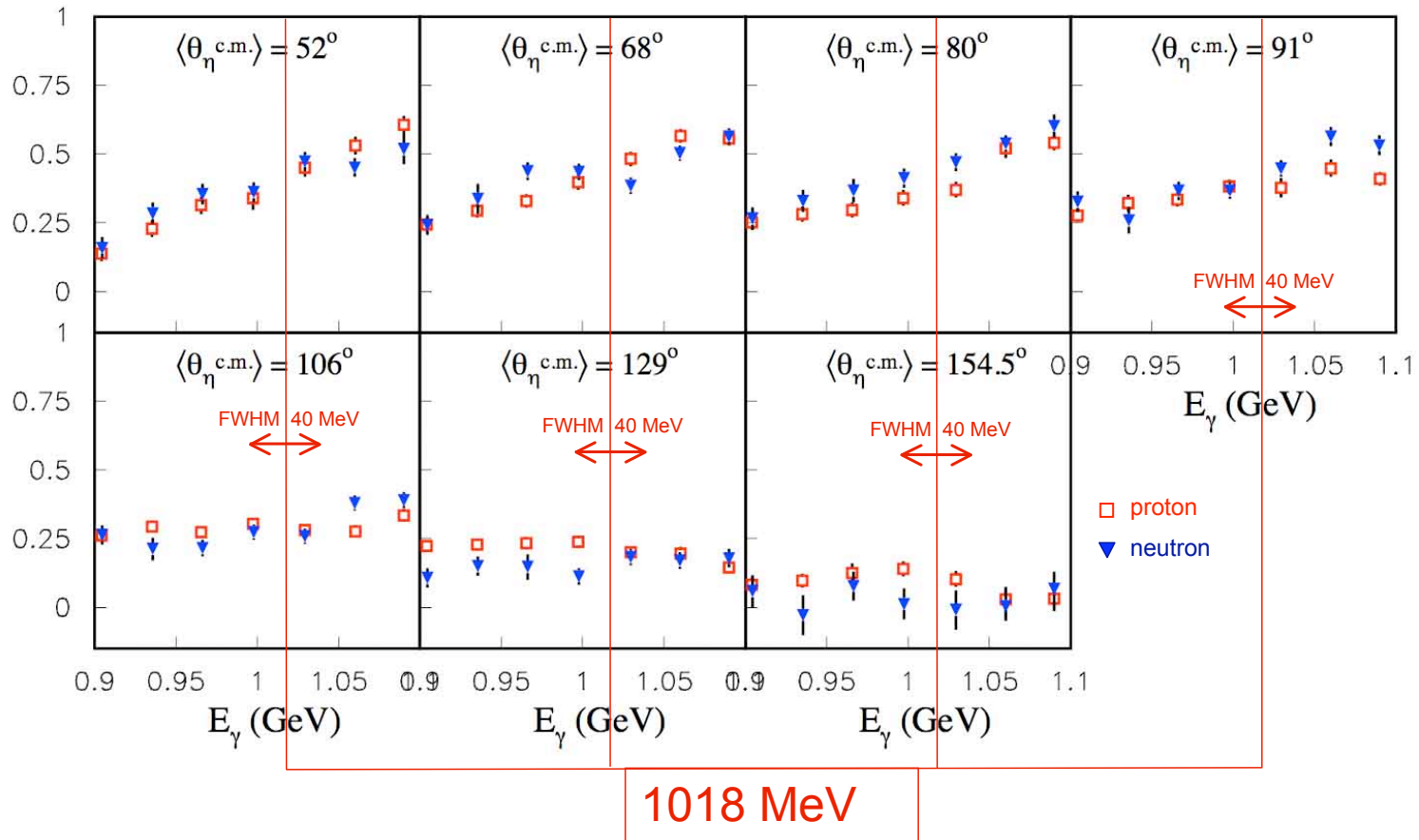
Asymmetry between 950 and 1100 MeV obtained with a narrow energy binning for various  $\eta$  center-of-mass angles. Comparison with the standard MAID model (dashed line), BCC partial-wave analysis (solid line) and predictions of the modified reggeized MAID model including a narrow P11 state. For this latter model, two versions are displayed corresponding to the two choices for the  $\zeta_{\eta N}$  hadronic relative phase (dot-dashed line:  $\zeta_{\eta N}=+1$ , dotted line:  $\zeta_{\eta N}=-1$ ).

# $\eta$ Asimmetry $\Sigma$ quasi-free p vs n

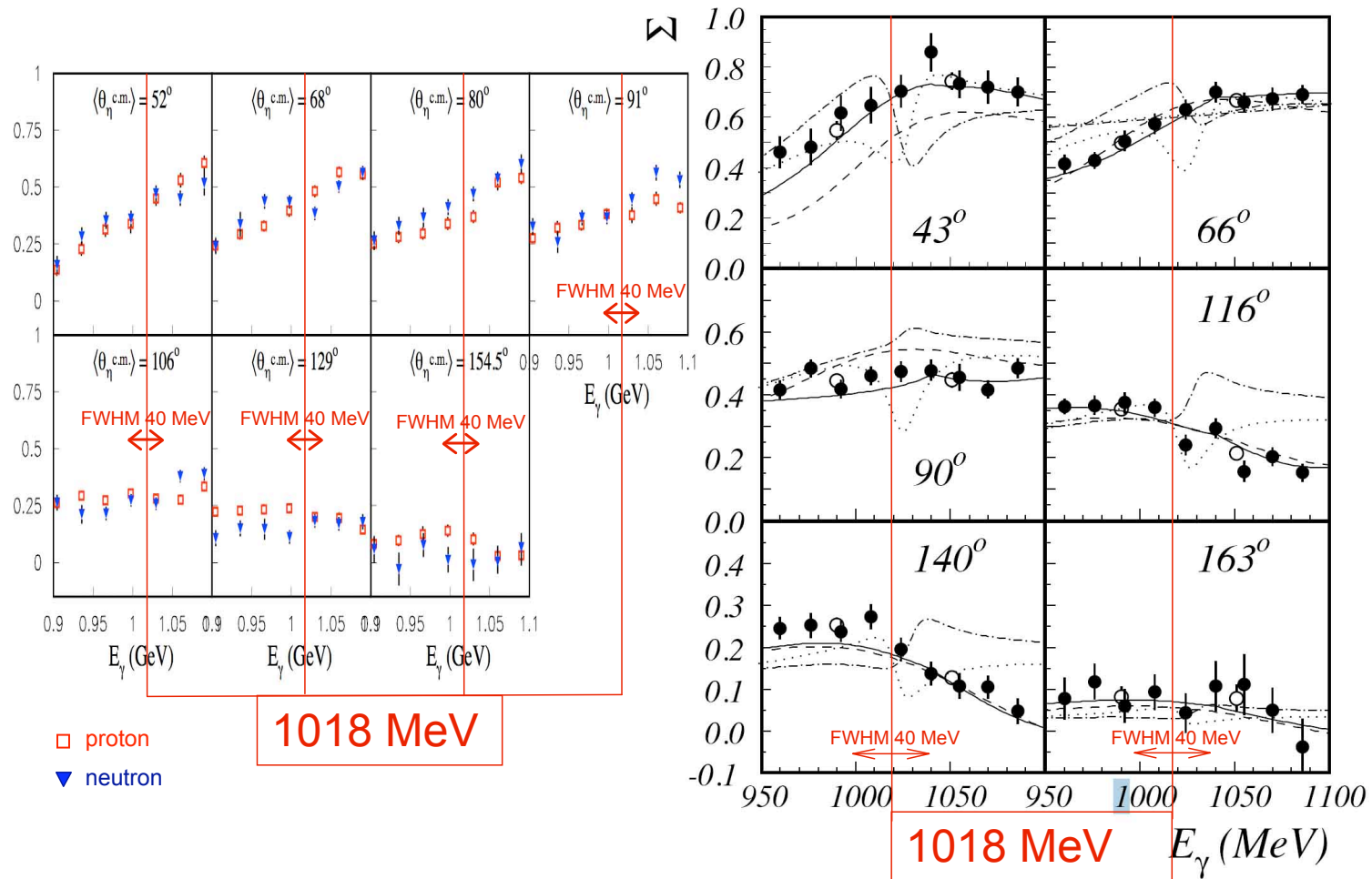




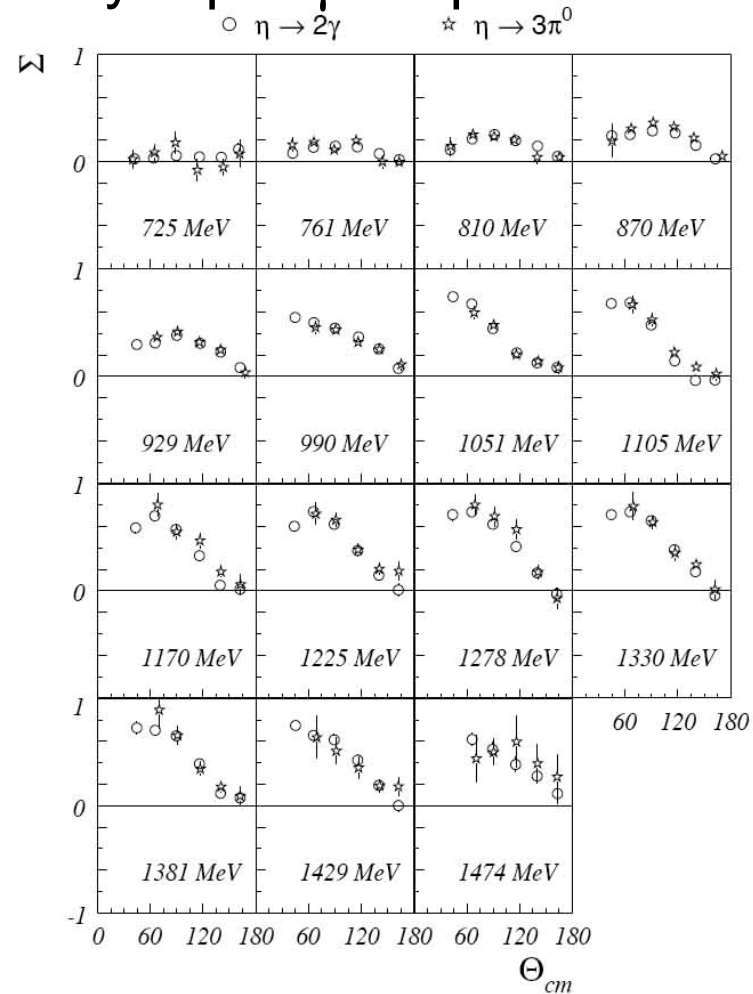
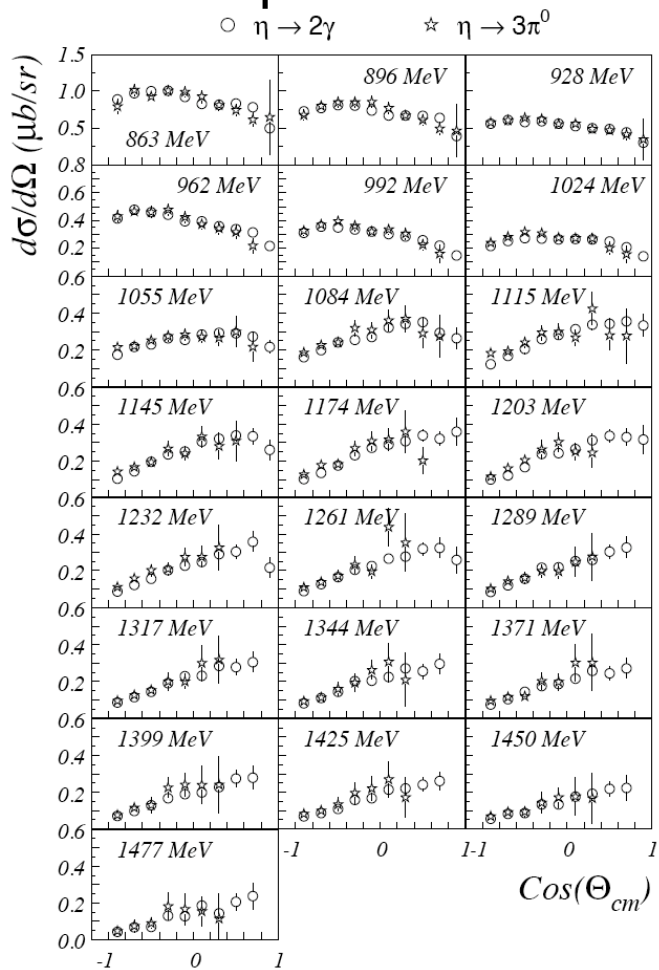
# $\eta$ Asimmetry $\Sigma$ quasi-free p vs n



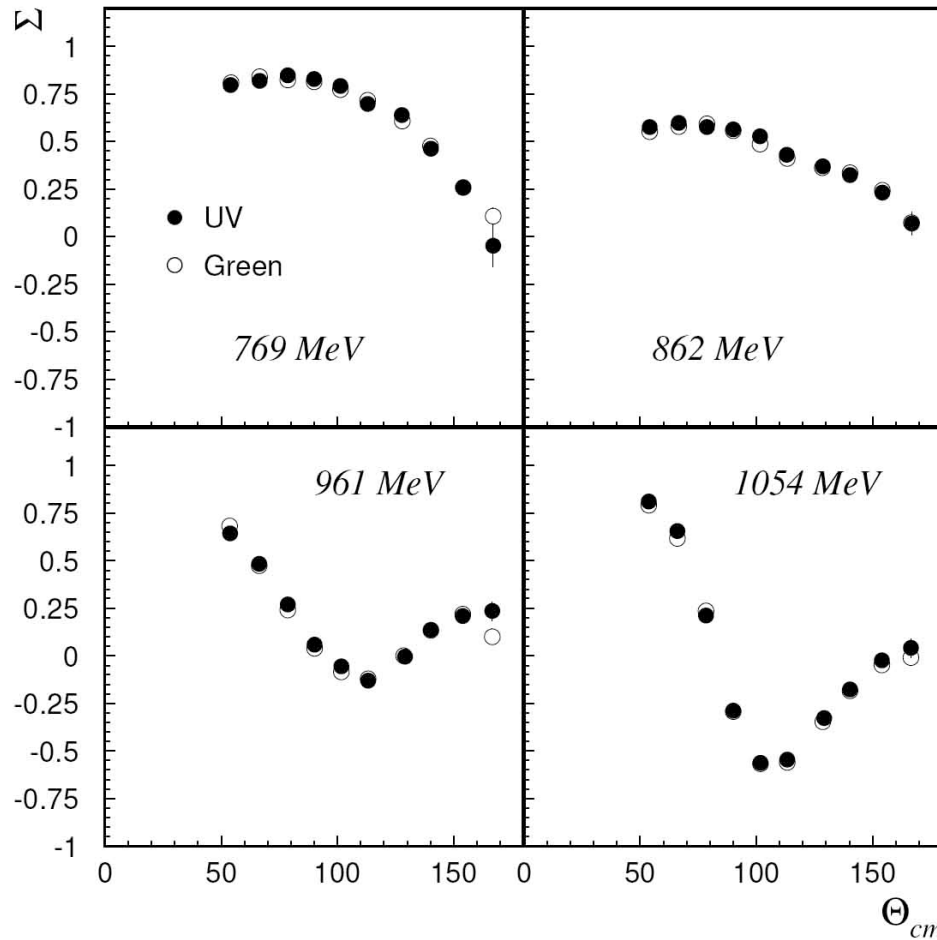
# $\eta$ Asimmetry $\Sigma$ quasi-free p/n and free p



# Free p - $d\sigma/d\Omega$ + Asimmetry - $\eta \rightarrow 2\gamma$ vs $\eta \rightarrow 3\pi^0$



## $\pi^0 p$ Asimmetry $\Sigma$ – Green vs UV



The asymmetry obtained with the Green laser line versus the UV is shown for the  $\gamma + p \rightarrow p + \pi^0$  reaction which has a large cross section.

$$\gamma + \mathbf{p} \rightarrow \omega + \mathbf{p}$$

We have analyzed two decay channels:

$$\gamma + \mathbf{p} \rightarrow \omega + \mathbf{p}$$

1.  $\omega \rightarrow \pi^0 + \gamma \rightarrow 3 \gamma$

2.  $\omega \rightarrow \pi^+ + \pi^- + \pi^0 \rightarrow \pi^+ + \pi^- + 2 \gamma$

The proton is detected in the BGO ball or in the forward detector.

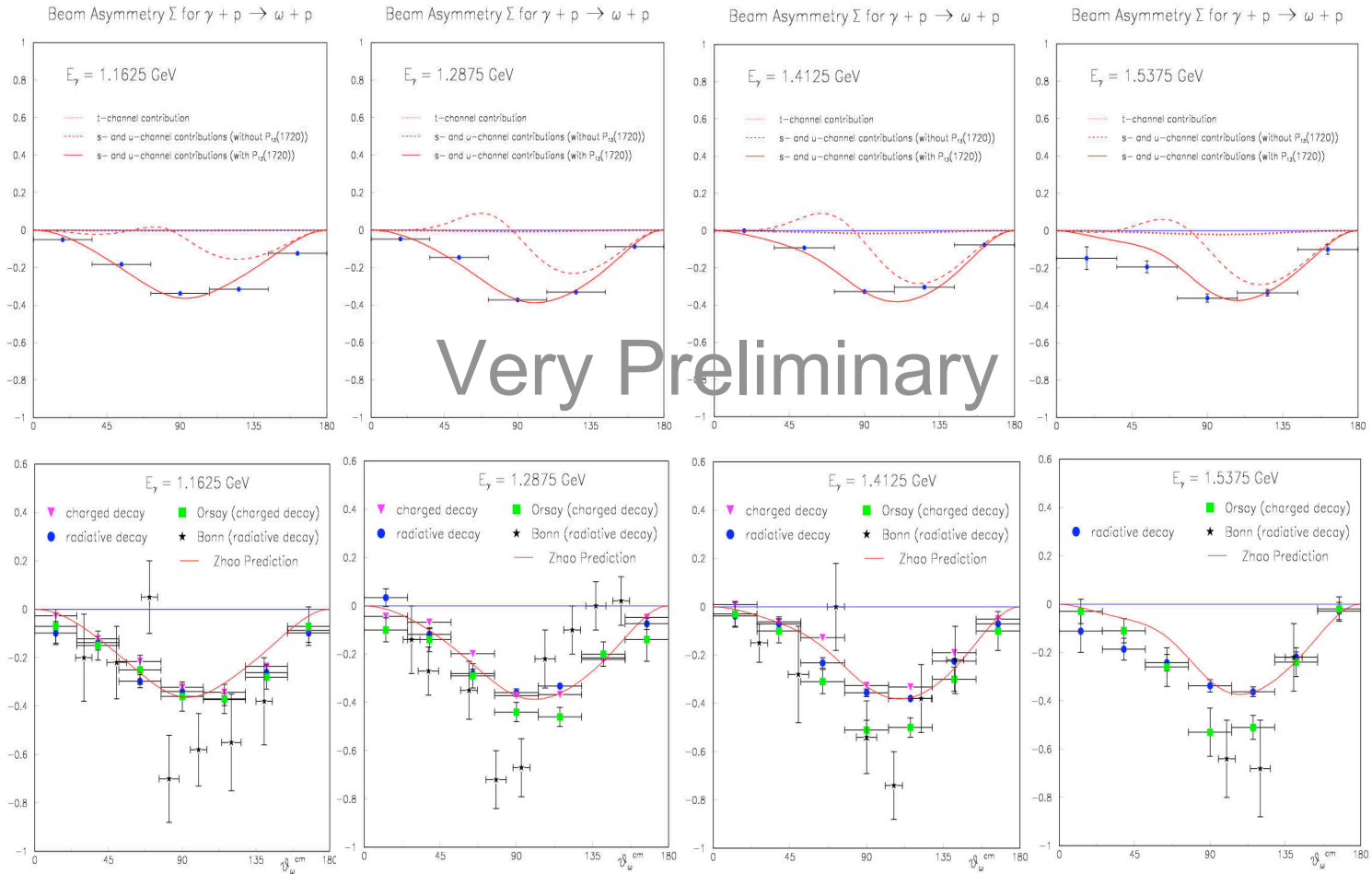
**Channel 1:** we require at least two photons in the BGO and the third one in the BGO or forward;

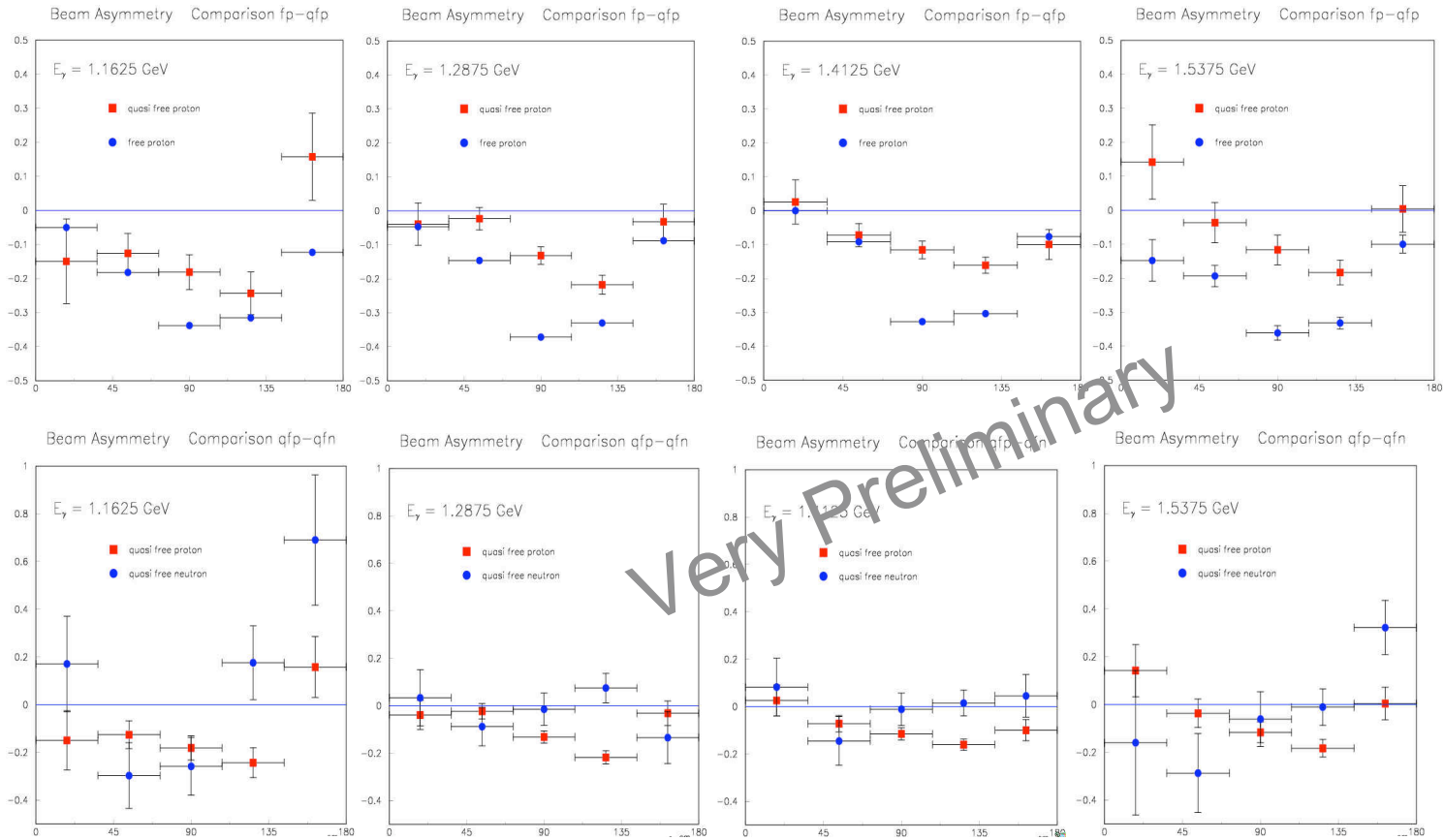
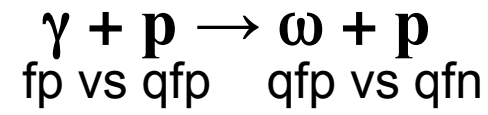
**Channel 2:** we require at least one photon in the BGO and the second photon and the two pions in the BGO or in the forward detector.

From the incident photon energy and proton momentum we calculate the missing mass of the other particles and compare with the  $\omega$  mass.

For channel 1 we calculate the invariant mass of the three photons and compare with the mass of the  $\omega$ . We apply the constraints of the two-body kinematics.

# $\gamma + p \rightarrow \omega + p$





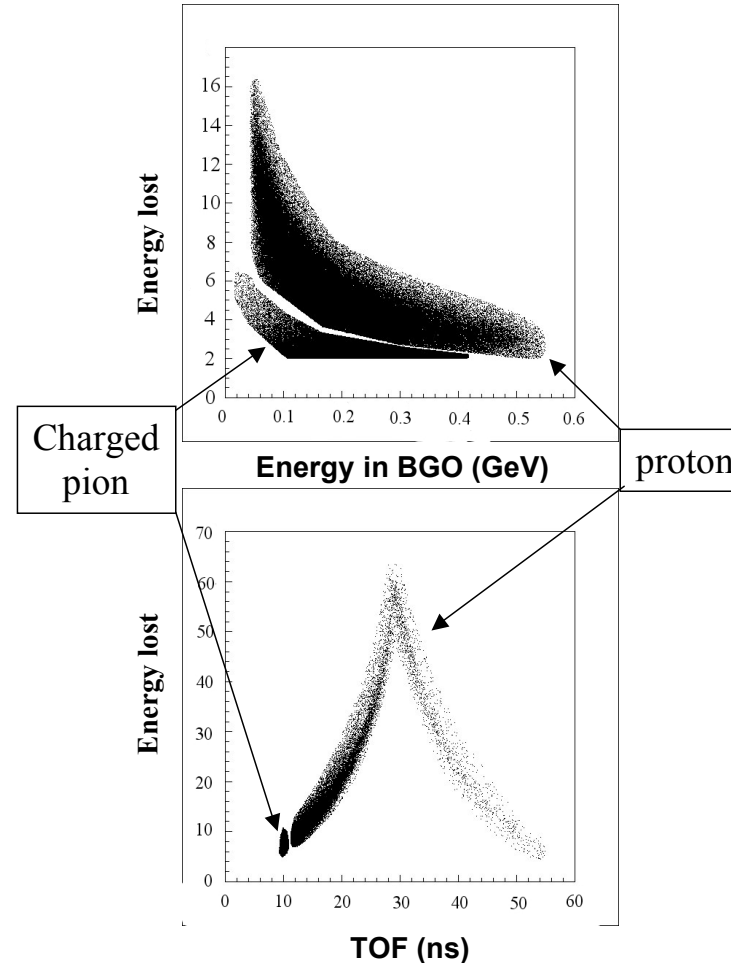
# $\gamma + n \rightarrow \pi^- + p$ Preliminary Event Selection

We identify charged particles by the coincidence of signals in three different detectors charged sensible.

We distinguish proton and pion in the central part of apparatus by bi-dimension cuts: energy lost in the BARREL versus energy released in the BGO.

We distinguish proton and pion in the forward part of apparatus by bi-dimension cuts: energy lost versus TOF of the scintillator wall .

In simulation, the number of the events generate by concurrent channel decreases at 14 % of the initial value applying the preliminary condition to have only one proton and only one pion in the apparatus.



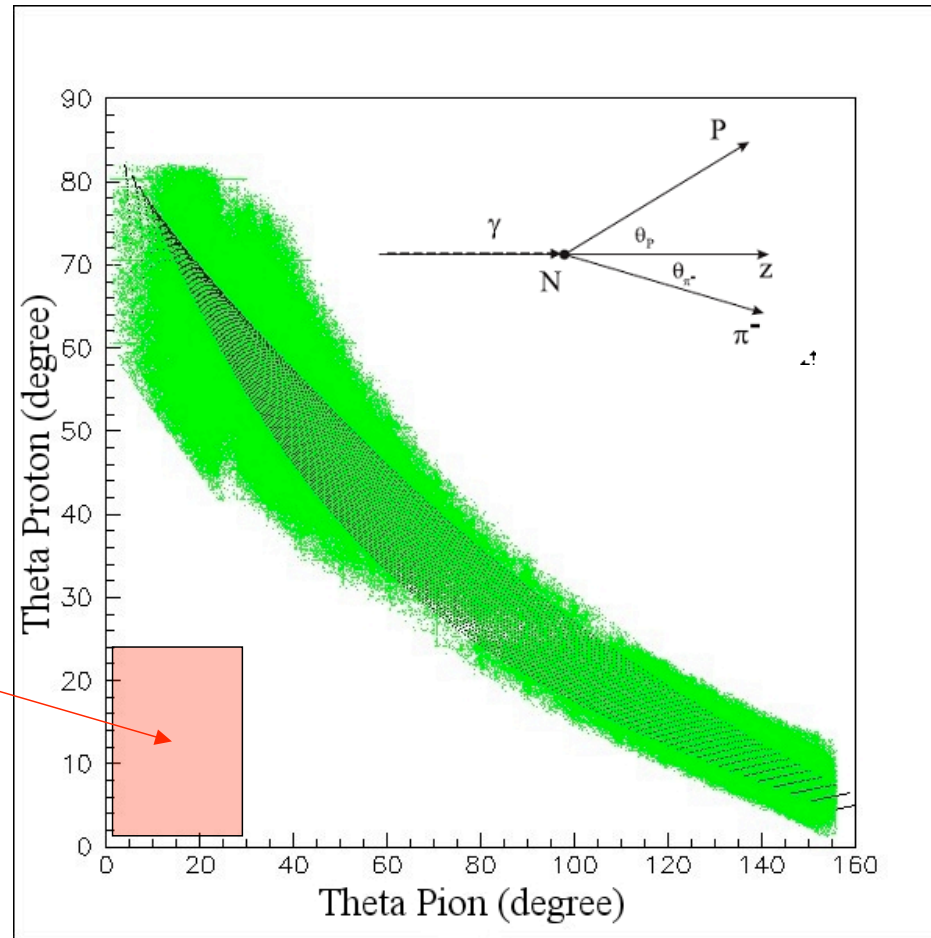


## Polar angle distribution of reaction products

Green: data

Black: kinematic calculation  
without any consideration on  
cross section of reaction.

No events with proton and pion  
in forward detectors at the same  
time are possible



# Hardware Conditions

We have used the following hardware conditions:

1. No other than one proton or one pion must be detected in the forward direction;
2. the energy,  $E^{\text{BGO}}$ , released in the calorimeter by particles detected only in the BGO must be lower than 5 MeV

# Cuts

- a) We combined the variables  $\Delta\theta = \theta_{\pi^-}^{calc} - \theta_p$  and  $R_p = E_p^{calc}/E_p^{measured}$  (see Fig a) ) selecting the events according to the condition

$$\frac{(x - \mu_x)^2}{\sigma_x^2} + \frac{(y - \mu_y)^2}{\sigma_y^2} - \frac{2C(x - \mu_x)(y - \mu_y)}{\sigma_x \sigma_y} < \sigma^2$$

where  $\sigma = 3$  and C is the correlation parameter

## Fit function

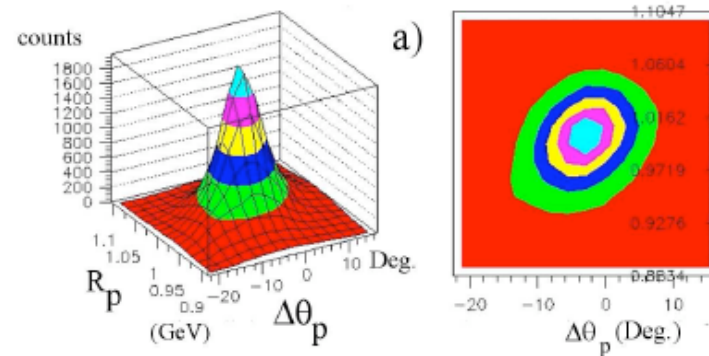
$$f(x, y) = \alpha + \beta \cdot e^{-\frac{1}{2}\gamma(x, y)}$$

$$\gamma(x, y) = \frac{A^2 - 2 \cdot Cor \cdot A \cdot B + B^2}{1 - Cor^2}$$

$$A = \frac{x - \bar{x}}{\sigma_x}$$

$$B = \frac{y - \bar{y}}{\sigma_y}$$

The parameters of the cuts a) and c) (next slide) were determined for different energy bin of gamma and for different periods of data acquisition.

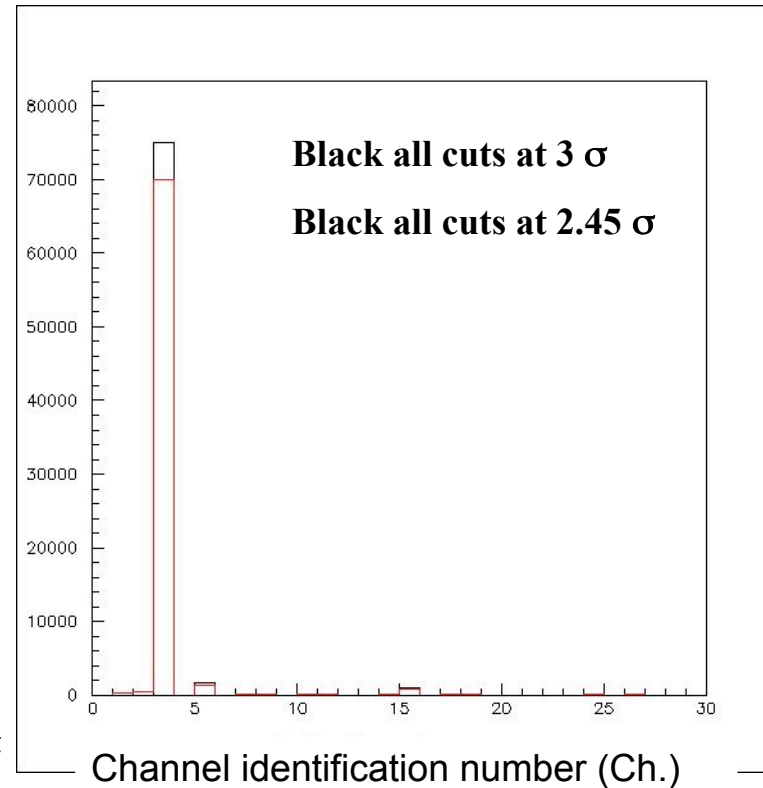


## Simulation: Signal and concurrent channels after cuts

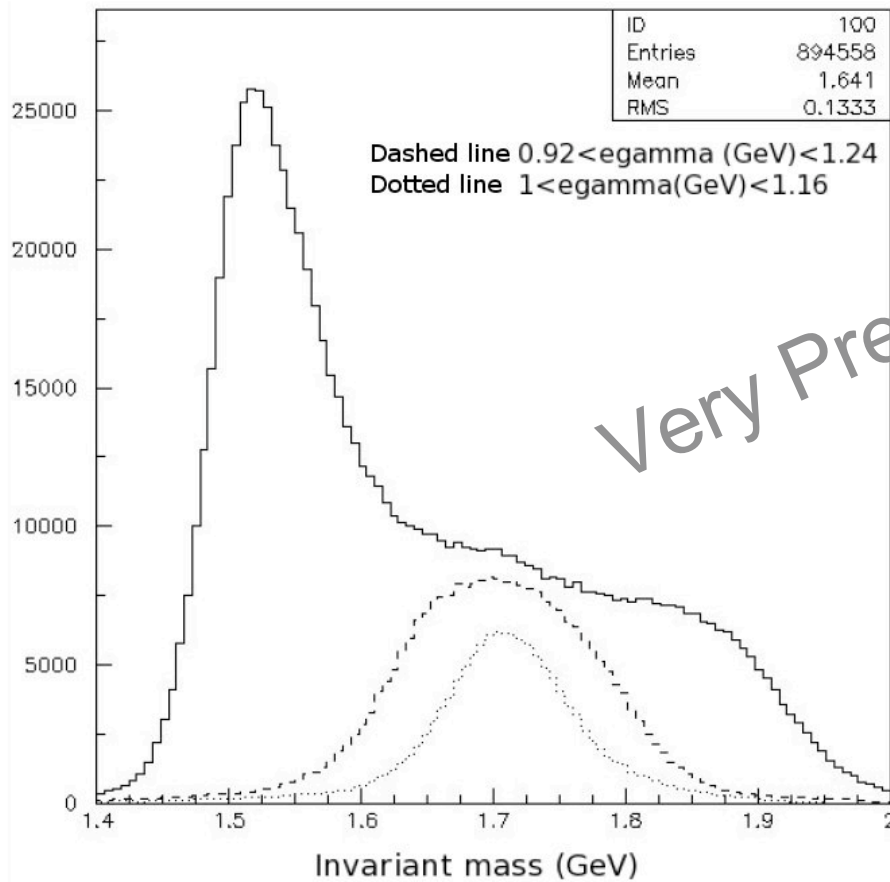
Ch. 3 =  $\gamma + n \rightarrow \pi^- p$  (signal)  
 Ch. 5 =  $\gamma + p \rightarrow \Delta^{++} \pi^-$   
 Ch. 8 =  $\gamma + n \rightarrow \Delta^+ \pi^-$   
 Ch. 10 =  $\gamma + n \rightarrow \Delta^- \pi^+$   
 Ch. 15 =  $\gamma + p \rightarrow \pi^+ \pi^- p$   
 Ch. 17 =  $\gamma + n \rightarrow \pi^+ \pi^- n$   
 Ch. 18 =  $\gamma + n \rightarrow \pi^0 \pi^- p$   
 Ch. 26 =  $\gamma + n \rightarrow \pi^+ \pi^- \pi^- p$

Ch.	Survival at $3 \sigma$	Survival at $2.45 \sigma$
<b>3</b>	<b>18.9%</b>	<b>17,8%</b>
<b>5</b>	<b>0.3%</b>	<b>0,2%</b>
<b>15</b>	<b>0.5%</b>	<b>0.4%</b>

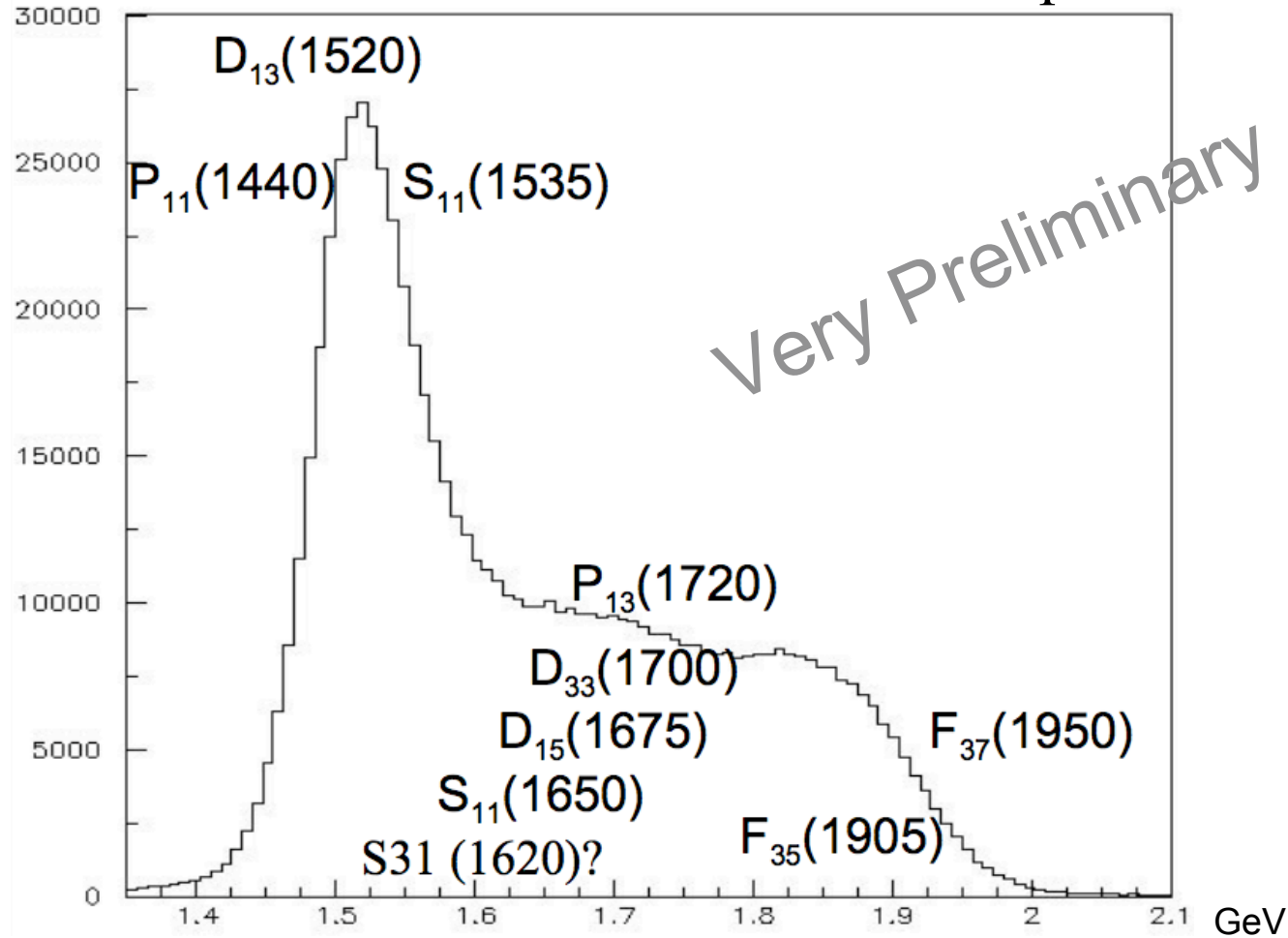
At  $3 \sigma$  the contribution of concurrent channels is lower than 2.3 %



# Invariant mass of the final state $\pi^- p$

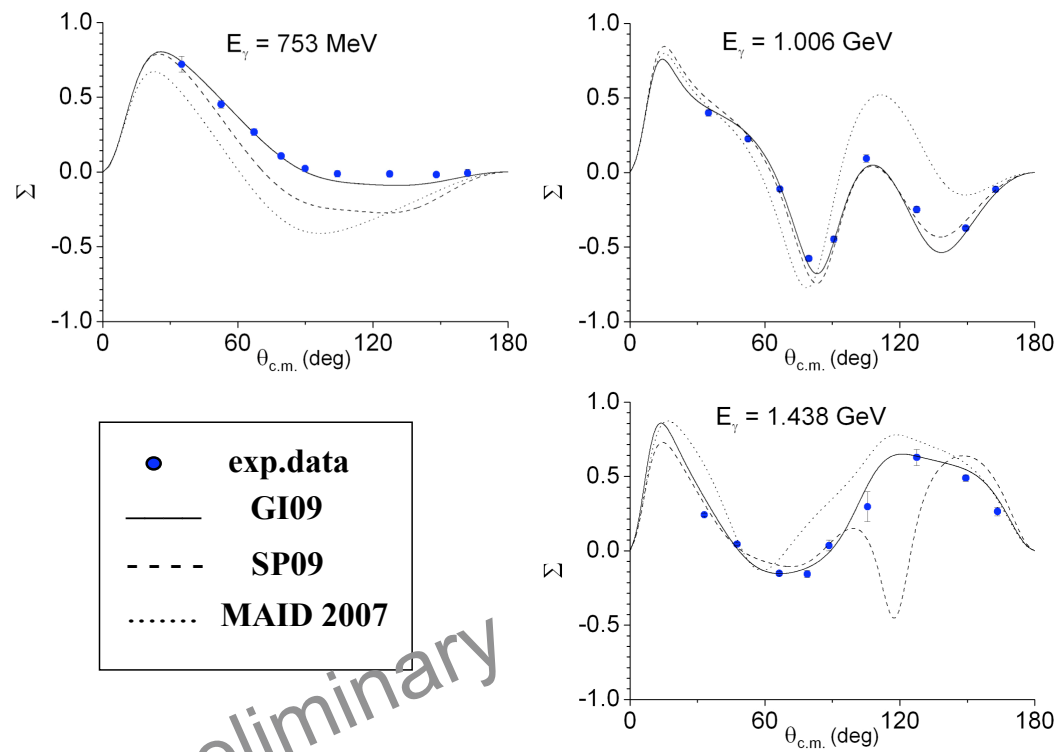


# Resonance contributions to the $\pi^- p$ final state



# $\pi^- p$ Beam Asymmetry $\Sigma$

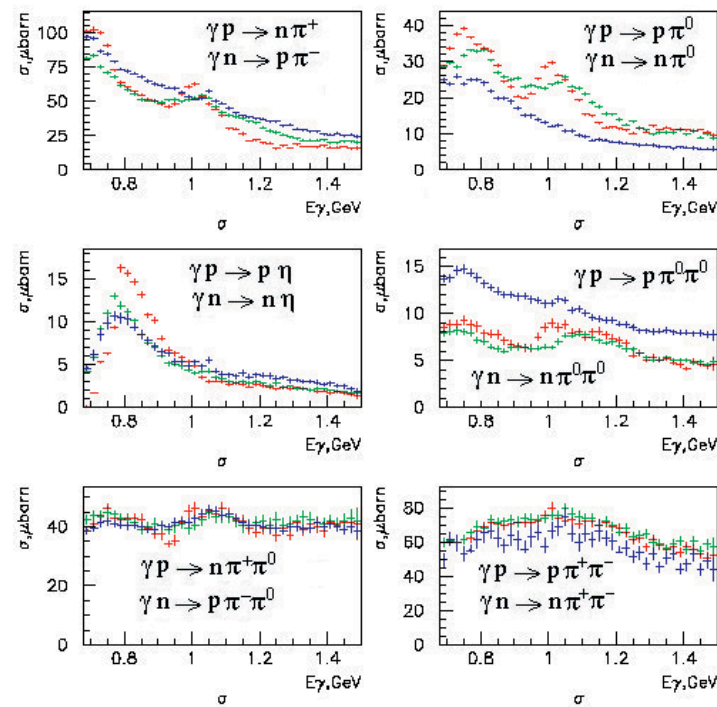
## Comparison between data and recent theoretical models



Very Preliminary

# INR - Total Cross Sections fp/qp/qfn

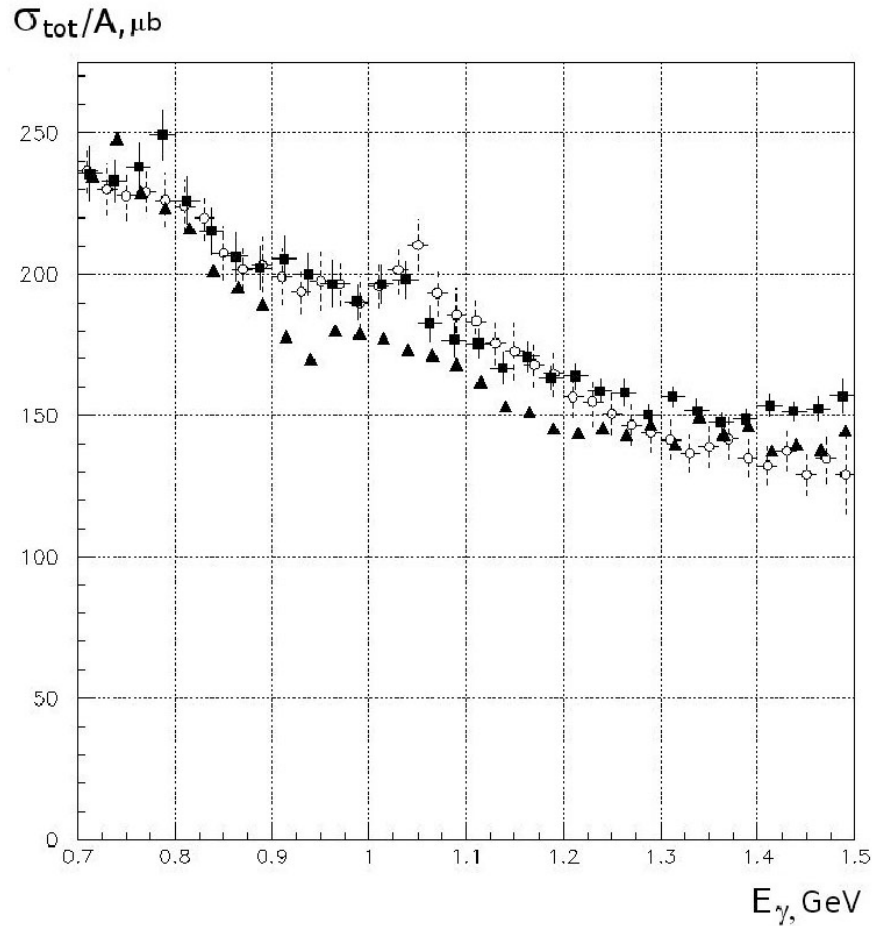
Partial cross sections for one and double pion and  $\eta$  meson photo-production on free and quasi-free proton and quasi-free neutron  
 Red – free proton, green – quasi-free proton, blue – quasi-free neutron.



Specific media modification in different channels indicates that two nucleon correlations plays important role in addition to Fermi motion.

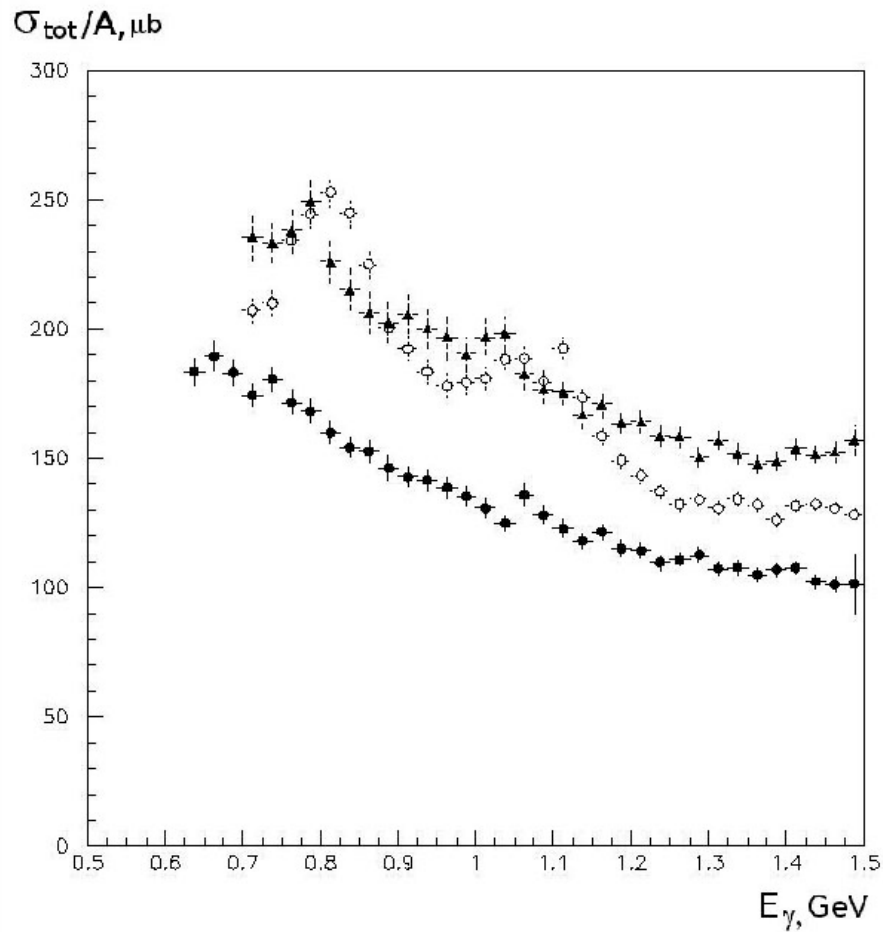


# INR - Total Cross Sections - Sub vs Sum



Total photo-absorption cross section for the deuteron, open and full points correspond to the subtraction and summing method, respectively. Full triangles are the result of Armstrong [2].

# INR - Total Cross Sections - p, d, C



Total Cross Sections per Nucleon for the proton (full triangles), deuteron (open points) and carbon (full points) targets:

- ▲ proton
- deuteron
- Carbon

# INR - CONCLUSIONS

1. Total cross sections obtained by subtraction and summing methods coincide within 5% error bars in the energy region up to 1.2 GeV. The discrepancy above this energy is explained by the triple meson production.
2. For neutron and proton we see the similar relative behavior and agreement in absolute scale, especially the presence of the F15 (1680) resonance in both cross sections in contradiction with the Armstrong (1972) results.
3. It is seen, that not only Fermi motion but also two nucleon correlations in the final state interaction is responsible for the modification of cross sections in the nuclear media.
4. Carbon cross section is practically coincides with the “universal curve” but lies in 30% below than the proton and deuteron one.